Molecular Photoscience Research Center International Workshop

Novel Magnetic Resonance Techniques in Millimeter and Terahertz Waves and their Applications to Bioscience" (MR-THz2016)

Abstract book

November 8-9, 2016
Rokkodai 2nd campus, Kobe University

Sponsors
Organization for Advanced and Integrated Research, Kobe University
Molecular Photoscience Research Center, Kobe University

Chairperson

Eiji Ohmichi (Kobe Univ.)
Hitoshi Ohta (Kobe Univ.)

Local Committee

Susumu Okubo (Kobe Univ.)
Takahiro Sakurai (Kobe Univ.)
Hideyuki Takahashi (Kobe Univ.)
Keisuke Tominaga (Kobe Univ.)

Scope

In this Workshop, novel magnetic resonance techniques in millimeter and terahertz waves and their applications to bioscience will be discussed. The aim of the Workshop is to focus on novel techniques and bioscience in magnetic resonance, and to combine them for better understanding of spin-related phenomena in biological systems. Main topics of this workshop are:

- Bio Imaging
- Distance Measurement
- Dynamic Nuclear Polarization
- Mechanically Detected Magnetic Resonance

Venue

Rooms Z201&Z202, Graduate School of Science, Rokkodai 2nd campus, Kobe University
1-1 Rokkodai-cho, Nada, Kobe, Hyogo 657-8501 Japan.

Banquet

Workshop banquet will be held on 8th of November at Japanese-style restaurant "Sakura" in Rokkodai 1st campus. (3rd floor of Academia Hall for Social Sciences, as indicated by No.8 in the map below)

Map

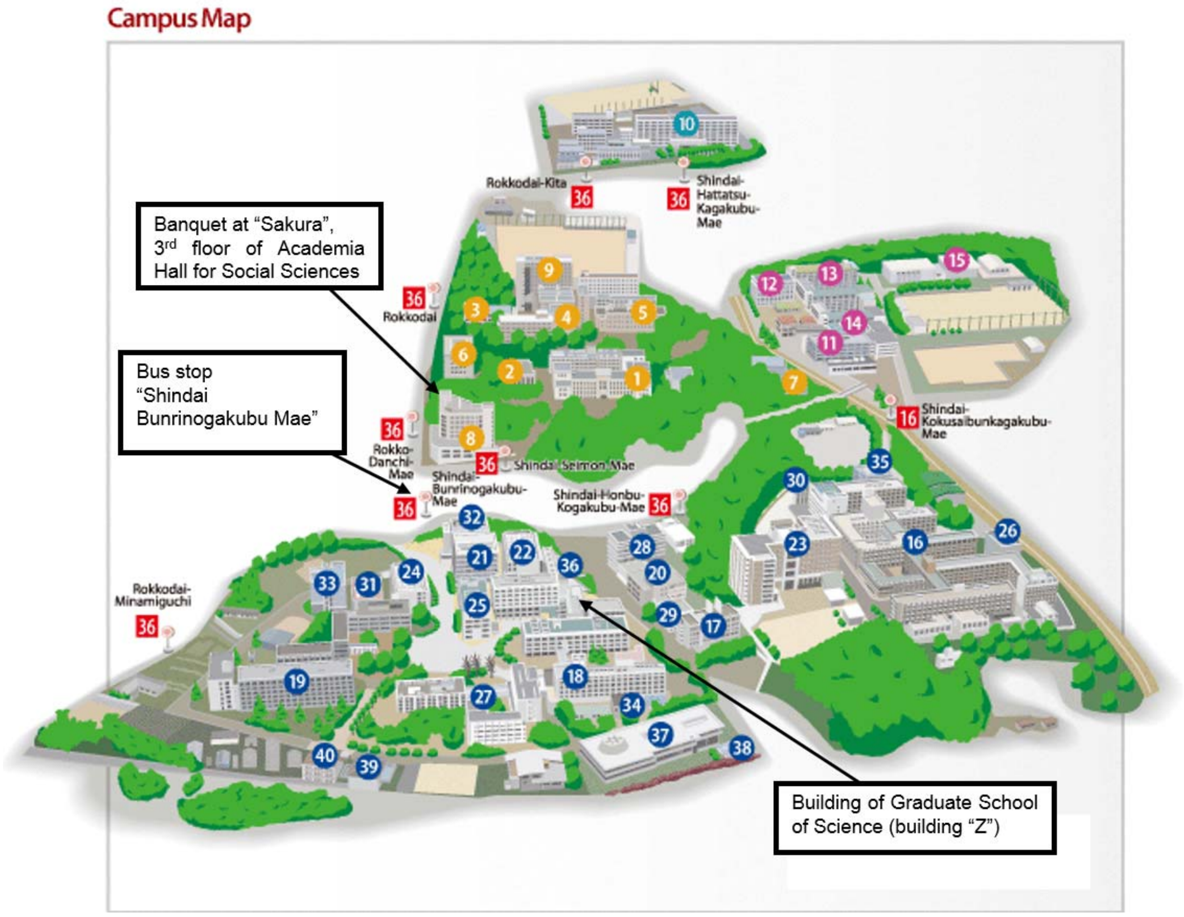

Access

Kobe University, Rokkodai 2nd Campus:
http://www.kobe-u.ac.jp/en/campuslife/campus_guide/campus/rokkodai2.html
(No. 82, building "Z")

- JR “Rokkomichi” station
  Kobe City Bus No.36, “Shindai Bunrinogakubu Mae”
- Hankyu ”Rokko” station
  Kobe City Bus No.36, “Shindai Bunrinogakubu Mae”

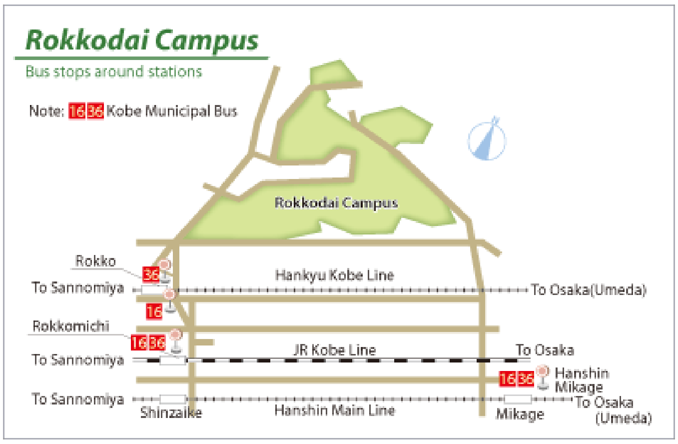

Presentation List

Plenary Lectures

PL-1 Gunnar Jeschke (ETH Zurich, Switzerland)

"What can EPR contribute to integrative structural biology?"

PL-2 Valery Khramtsov (West Virginia University, USA)

"Multifunctional EPR-based spectroscopy and imaging of local chemical microenvironment"

PL-3 Konstantin Ivanov (International Tomography Center, Russia)

"Nuclear spin hyperpolarization and level anti-crossings"

PL-4 Christopher Kay (University College London, UK)

"EPR studies of photoexcited paramagnetic states in polymers, single crystals and thin films"

Invited Talks

T-1 Toshikazu Nakamura (IMS)

"Pulsed and muti-frequency ESR study for material and biological sciences"

T-2 Yasuhiro Kobori (Kobe Univ.)

"Geometry and electron tunneling route of photoinduced primary charge-separated state in the photosynthetic reaction center"

T-3 Kazuyuki Takeda (Kyoto Univ.)

"Converting NMR signals into light via a membrane capacitor"

T-4 Masaya Toda (Tohoku Univ.)

"Magnetic resonance force measurement by high sensitive Si cantilever with a magnet particle"

T-5 Hideyuki Takahashi (Kobe Univ.)

"The development and application of force-detected THz-ESR measurement system"

T-6 Hiroshi Hirata (Hokkaido Univ.)

"Development of CW-EPR-based oxygen mapping using dicarboxy-PROXYLs and single-point imaging modality"

T-7 Kazuhiro Ichikawa (Kyushu Univ.)

"Development of DNP-MRI scanners at wide frequency range for biomedical application -from skin to large animal-"

T-8 Toshimichi Fujiwara (Osaka Univ.)

"Dynamic nuclear polarization with double 460 GHz gyrotrons for the sensitivity enhancement of magic-angle-spinning NMR at 30 K"

T-9 Toshiaki Arata (Osaka Univ.)

"Application of distance determination using spin labeling dipolar EPR spectroscopy to complex protein system: 3-dimensional organization and regulatory action of troponin-tropomyosin in muscle thin filament"

T-10 Hiroyuki Mino (Nagoya Univ.)

"Local structure of photosystem II revealed by pulsed ELDOR"

T-11 Masaki Horitani (Northwestern Universtiy, USA)

"ENDOR reveals how radical SAM enzymes tame highly reactive radical"

T-12 Raivo Stern (National Institute of Chemical Physics and Biophysics, Estonia)

"*Novel possibilities in solid state NMR: cryoMAS down to 10 K and NMR in pulsed magnetic fields up to 70 T*"

Poster Presentations

P-1 Takayuki Suzuki (JEOL Resonance)

"A study of ESR chromatography by means of the inverse transformation"

P-2 Fumitoshi Ema (Kobe Univ.)

"Time-resolved EPR study on the photoreaction and radical dynamics of 9,10-anthraquinone-2,6-disulfonate and ascorbic acid at bilayer interface"

P-3 Reina Minobe (Kobe Univ.)

"Time resolved EPR study on the orientation of the primary charge separated state of the quinone-depleted PSII reaction center"

P-4 Tsubasa Okamoto (Kobe Univ.)

"Terahertz ESR measurement of metalloporphyrin complexes"

P-5 Toshihiro Miki (Kobe Univ.)

"Fabrication of Fabry-Perot type cantilever for high-sensitivity force-detected ESR measurement"

P-6 Akikazu Miyazaki (Kobe Univ.)

"Development of a piezoelectric translational stage for magnetic resonance force microscopy"

P-7 Hidekazu Horie (Kobe Univ.)

"Development of a microforce measurement apparatus using a cantilever"

P-8 Masaya Fujimoto (Kobe Univ.)

"ESR study of kagome like frustrated magnet $K_2Mn_3(OH)_2(VO_4)_2$*"*

P-9 Akihiko Takahashi (Kobe Univ.)

"Spin dynamics of two-dimensional square lattice magnet $Sr_2MnO_2Cl_2$*"*

P-10 Daisuke Miyazaki (Kobe Univ.)

"Submillimeter wave ESR measurements of S=1/2 distorted diamond chain $Cu_3(OH)_2(CH_3CO_2)_2(H_2O)_xX_y$*"*

P-11 Arata Morimitsu (Kobe Univ.)

"Terahertz ESR measurements of multiferroic compound $BiFe_{0.9}Co_{0.1}O_3$*"*

P-12 So Kubota (Kobe Univ.)

"High Frequency ESR Measurements of S=1/2 antiferromagnetic chain $KCuMoO_4(OH)$*"*

P-13 Yuki Hirao (Kobe Univ.)

"High pressure THz ESR measurements of spin-gap system $KCuCl_3$*"*

P-14 Eito Oki (Kobe Univ.)

"Development of high pressure and high field ESR system and its application to quantum spin system"

P-15 Khalif Benzid (Kobe Univ.)

"ESR study of nonmagnetic impurity effect of S=1/2 two legs spin ladder antiferromagnet $[Ph(NH_3)](18\text{-crown-}6)[Ni(dmit)_2]_{1-x}[Au(dmit)_2]_x$*"*

Time table of MR-THz2016

time	Nov. 8 (Tue)	Nov. 9 (Wed.)
8:30		
		T-6 H. Hirata (30min) 8:45-9:15
9:00		
		PL-2 V. Khramtsov (40 min) 9:15-9:55
10:00		T-7 K. Ichikawa (30min) 9:55-10:25
		break
		PL-3 K. Ivanov (40min) 10:40-11:20
11:00		
		T-8 T. Fujiwara (30min) 11:20-11:50
		lunch 11:50-13:00
12:00		
13:00	Opening (Ohmichi)	Poster session 13:00-14:00
	PL-1 G. Jeschke (40 min) 13:20-14:00	
14:00	T-1 T. Nakamura (30 min) 14:00-14:30	PL-4 C. Kay (40 min) 14:00-14:40
	T-2 Y. Kobori (30 min) 14:30-15:00	
		T-9 T. Arata (30min) 14:40-15:10
15:00	break	
	T-3 K. Takeda (30min) 15:10-15:40	T-10 H. Mino (30min) 15:10-15:40
	T-4 M. Toda (30min) 15:40-16:10	T-11 M. Horitani (30min) 15:40-16:10
16:00		
	T-5 H. Takahashi (30min) 16:10-16:40	T-12 R. Stern (30min) 16:10-16:40
	break	Closing (Ohta) 16:40-17:00
	Facilities presentation 16:50-17:10	
17:00		
	Lab. Tour (60 min) 17:10-18:10	40min-talk 4 30min-talk 12
18:00		
	move to Sakura	
	Banquet Restaurant "Sakura" 18:30-20:30	
19:00		
20:00		

What can EPR contribute to integrative structural biology?

G. Jeschke

[1]*Department of Chemistry and Applied Biosciences, ETH Zürich, CH-8093 Zürich, Switzerland.*

Email: gjeschke@ethz.ch

For decades, structural biology was dominated by the idea that the monomer sequence of a biomacromolecule encodes a single well-defined ground state conformation, the “native state” of a protein or RNA. During the past few years it has become more and more clear that function of proteins and RNAs depends on dynamical exchange between different conformations and on disorder-order transitions, i.e., on intrinsic disorder in certain states of the macromolecules in a living cell. Such a more complex structural landscape cannot be fully characterized by established techniques with atomistic resolution, such as x-ray crystallography or high-resolution NMR spectroscopy. In fact, no single experimental technique may be able to provide sufficient information to establish a reasonable model, whereas computational techniques may run into limitations of sampling and of force field accuracy.

Integrative structural biology is the attempt to overcome this problem by integrating information from multiple experimental and computational techniques into a single model of the system. To avoid artificial bias, this requires that accuracy and precision of the restraints are known. Here I discuss how long-range distance distribution restraints (DDRs) and water accessibility restraints are obtained by combining EPR techniques with site-directed spin labeling of proteins and RNA and what is known about the precision and accuracy of such restraints. For DDRs, an error analysis is required for the ill-posed problem of converting time-domain data to distance distributions and the uncertainty of predictions of the conformational distribution of the spin label itself must be known. The latter uncertainty is quantified by statistical analysis of a large set of experimental data and visualized by multilateration of the spin label position for proteins with a known structure. For the active state of pro-apoptotic protein Bax multilateration of spin label positions in a disordered domain provides information on the orientation of this pore-lining protein with respect to the mitochondrial membrane [1]. Furthermore, it is shown how well an ensemble of conformations can be characterized by a limited number of DDRs [2]. For lanthanide labels, it is demonstrated that NMR pseudo-contact shift data allow for an improved characterization of the spatial distribution of the label.

Water accessibility restraints can be derived from the electron spin echo envelope modulation (ESEEM) depth of matrix deuterons, after exchange of the water by heavy water, through measurements at cryogenic temperatures. Although such data can be directly related to a local concentration profile of deuterons, it has limited precision. In Overhauser dynamic nuclear polarization (DNP), polarization is transferred from the electron spin of the label to water protons which are then detected by NMR. With this experiment, no isotope substitution is required and measurements can be performed at physiological temperatures. Theoretical description of the polarization transfer is much more involved than theoretical description of ESEEM. However, for the spin-labelled membrane-inserting peptide WALP23 it was found that data from this technique is in surprisingly good agreement with the equilibrium water concentration profile in a DOPC bilayer.

[1] S. Bleicken, G. Jeschke, C. Stegmüller, R. Salvador-Gallego, A.J. García-Sáez, E. Bordignon, Mol. Cell **56** (2014) 496.
[2] G. Jeschke, Proteins **84** (2016) 544.
[3] T. F. Segawa, M. Doppelbauer, L. Garbuio, A. Doll, Y. O. Polyhach, G. Jeschke, J. Chem. Phys. (2016) 144, 194201.

PL-2

Multifunctional EPR-based spectroscopy and imaging of local chemical microenvironment

V.V. Khramtsov[1]

[1]*West Virginia University, In Vivo Multifunctional Magnetic Resonance center, Robert C. Byrd Health Sciences Center, Morgantown, WV 26506, USA*

Email: valery.khramtsov@hsc.wvu.edu

A need in quantitative mapping of critical parameters of local chemical microenvironment in biological systems, especially in vivo, with spatial and temporal resolution is emerging. In particular, tissue oxygenation, acidosis, redox and GSH content are physiologically important markers of the processes related to tumorigenesis characterizing cancer progression, aggressiveness and efficacy of tumor microenvironment (TME)-targeted anticancer therapy. Among the other chemical parameters of TME recently identified as important signaling molecule in tumorigenesis is inorganic phosphate, Pi. EPR-based spectroscopy and imaging in combination with functional paramagnetic probes provide non-invasive analytical tools for assessment of local chemical microenvironment. In particular, stable organic radicals involved in reversible exchange processes may allow for quantitative measurements of the kinetic and thermodynamic parameters of the corresponding chemical reactions as illustrated in Figure 1 for multifunctional oxygen (pO_2)-, pH- and Pi-sensitive trityl probe [1,2].

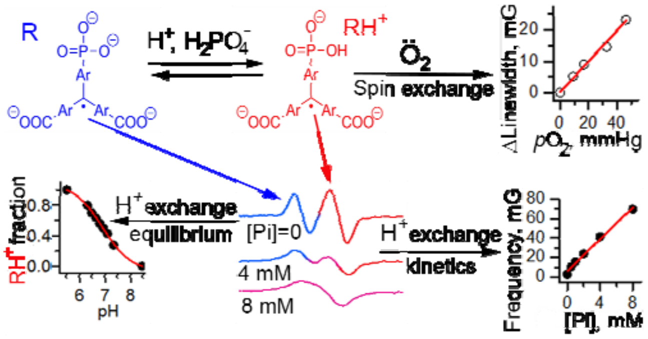

Fig. 1. Multifunctional assessment of chemical microenvironment using trityl probe. pH-dependent equilibrium between two ionization states of the probe and their corresponding high-field components of the EPR spectrum are shown. The EPR linewidth is a pO_2 marker (accuracy, ≈ 1 mmHg; pO_2 range, 1-100 mmHg). The fraction of protonated state is a pH marker in the range from 6 to 8.0 (accuracy, ± 0.05). Proton exchange rate (extracted by spectra simulation and expressed in mG) is a marker of Pi concentration (accuracy of [Pi] assessment, ± 0.1 mM, range, 0.1-20 mM).

We demonstrated that currently available soluble nitroxide and trityl probes can be efficiently used for multifunctional assessment of chemical microenvironment in living tissues providing new insights in the underlying biochemical and physiological processes. In this work, we employ recently developed multifunctional paramagnetic probes in combination with L-band EPR spectroscopy and Overhauser-enhanced MRI (OMRI) for *in vivo* concurrent assessment of the chemical parameters in TME of various mouse models of cancer. While the data support the existence of hypoxic and acidic regions in TME, the most dramatic differences, about 2-fold higher concentrations in tumors vs. normal tissues, were observed for interstitial [Pi] - the only parameter that also allowed for discrimination between non-metastatic and highly metastatic tumors. Correlation analysis between [Pi], pO_2, pH_e and tumor volumes reveal an association of high [Pi] with changes in bioenergetic status and supports different mechanisms of protons and Pi accumulation in TME. The proposed future methodological developments include advances in the synthesis of multifunctional paramagnetic probes and progress in EPR-based imaging techniques such as rapid scan (RS) EPR imaging and Overhauser-enhanced MRI.

Supported by NIH grants CA194013, CA192064 and U54GM104942

[1] Bobko AA, Dhimitruka I., Zweier JL. and Khramstov VV. *Angew. Chem. Int. Edit.*, **53** (2014) 2735-2738.

[2] Dhimitruka I, Bobko AA, Eubank TD, Komarov DA, and Khramtsov VV. *J. Amer. Chem. Soc.*, **135** (2013), 5904−5910.

The role of level anti-crossings in nuclear spin hyperpolarization

Andrey. N. Pravdivtsev,[1,2] Alexandra. V. Yurkovskaya,[1,2] Robert Kaptein,[4]
Hans Heinrich Limbach,[3] Hans-Martin Vieth,[1,3] Konstantin. L. Ivanov[1,2]

[1] *International Tomography Center, Novosibirsk, Russia*

[2] *Novosibirsk State University, Novosibirsk, Russia*

[3] *Freie Universität Berlin, Berlin, Germany*

[4] *Utrecht University, Utrecht, the Netherlands*

Email: ivanov@tomo.nsc.ru

In hyperpolarization experiments, it is often desirable to transfer the initial polarization to other nuclei of choice, either protons or insensitive nuclei such as ^{13}C and ^{15}N. This situation arises primarily in Chemically Induced Dynamic Nuclear Polarization (CIDNP), Para-Hydrogen Induced Polarization (PHIP), and the related Signal Amplification By Reversible Exchange (SABRE). Here we discuss polarization transfer mechanisms, in particular focusing on the role of Level Anti-Crossings (LACs) therein.

So-called "spontaneous" polarization transfer may occur both at low and high magnetic fields. In addition, transfer of spin polarization can be accomplished by using especially designed pulse sequences. It is now clear that at low field spontaneous polarization transfer is primarily due to coherent spin-state mixing under "strong coupling" conditions. However, thus far the important role of LACs in this process has not received much attention. Another promising high-field technique is to generate the strong coupling condition by spin locking using strong radio-frequency fields. Here, an analysis of polarization transfer in terms of LACs in the rotating frame is very useful to predict which spin orders are transferred depending on the strength and frequency of the B_1 field. Finally, the key role of LACs in SABRE experiments is discussed.

Acknowledgements

This work has been supported by the Russian Foundation for Basic Research (projects No. 14-03-00397 and 15-33-20716), the Russian Science Foundation and the Alexander von Humboldt Foundation. K.L.I. acknowledges support from the Japanese Society for the Promotion of Science (JSPS).

Combining EPR distance measurements with X-Ray Crystallography and Molecular Modeling: A Robust Toolbox?

Christopher W. M. Kay[1,2]

[1]Institute of Structural and Molecular Biology, University College London, Gower Street, London WC1E 6BT, UK.

[2]London Centre for Nanotechnology, University College London, 17-19 Gordon Street, London WC1H 0AH, UK.

Email: c.kay@ucl.ac.uk

Structural biology relies on high-resolution methodologies to reveal protein function, mis-function and disease. X-ray crystallography, NMR spectroscopy and electron microscopy are three principal techniques used for this purpose. However, advances in other areas such as EPR spectroscopy are emerging as complementary approaches for unraveling details of cellular processes at the molecular level. A form of pulsed EPR spectroscopy known as PELDOR or DEER allows the dipolar interaction between pairs of paramagnetic centers to be determined in frozen solution over the range 2-10 nm. In this talk, I will discuss some of our work in this area. In some systems, native centers such as flavin radicals [1] or Cu^{2+} [2] or can be used as labels, but because the majority of proteins are diamagnetic, nitroxide spin labels are usually attached to proteins via native or engineered cysteine residues. We have combined X-ray crystallography, EPR-based distance measurements between nitroxide spin labels and molecular modeling/dynamics simulations to reveal structural and functional details of both membrane and soluble proteins [3-6]. Finally, we have recently suggested an approach for improving the sensitivity of the DEER experiment [7].

This work is supposed by BBSRC, MRC, Wellcome Trust and UCL.

[1] Kay et al. (2006). Determination of the Distance between the Two Neutral Flavin Radicals in Augmenter of Liver Regeneration by Pulsed ELDOR. **J. Amer. Chem. Soc**. 128 76-77.

[2] Kay et al. (2007). Pulsed ELDOR determination of the intramolecular distance between the metal binding sites in Dicupric human serum transferrin and lactoferrin. **J. Amer. Chem. Soc.** 129 4868-4868.

[3] Phan et al. (2011) Crystal structure of the FimD usher bound to its cognate FimC:FimH substrate **Nature** 474 47-53.

[4] Bagnéris et al. (2013) Role of the C-Terminal Domain in the Structure and Function of Tetrameric Sodium Channels. **Nature Comms**. 4:2465.

[5] Bagnéris et al. (2015) Probing the Solution Structure of IκB Kinase (IKK) Subunit γ and its Interaction with Kaposi's Sarcoma Associated Herpes Virus Flice Interacting Protein and IKK Subunit β by EPR Spectroscopy. **J. Biol. Chem**. 290 16539-16549.

[6] Papaioannou et al. (2016) Structural and biophysical investigation of the interaction of a mutant Grb2 SH2 domain (W121G) with its cognate phosphopeptide. Protein Science 25 627-637

[7] Salvadori et al. (2015) Exploiting the symmetry of the resonator mode to enhance PELDOR sensitivity. **Appl. Magn. Reson.** 46 359-368.

Pulsed and Multi-frequency ESR Study for Material and Biological Sciences

T. Nakamura[1,2]

[1] *Institute for Molecular Science, Myodaiji, Okazaki 444-8585, Japan.*

[2] *SOKENDAI, Myodaiji, Okazaki 444-8585, Japan.*

Email: ohmichi@harbor.kobe-u.ac.jp

Multi-frequency and pulsed ESR measurements are advantageous for studying fundamental electronic properties of molecular functional materials and for understanding the structural dynamics of bio-functional materials. Developing of the advanced ESR technique enables us to perform detailed electronic investigations of functional materials, and structural investigations of bio-functional materials. We performed multi-frequency (X-, Q-, and W-bands) and pulsed ESR measurements (photo-induced time-resolved ESR (TR-ESR), pulsed electron-electron double resonance (PELDOL),) on a) organic conductors, b) photoconductive materials, c) functional polymers, and d) bio-functional materials so far [1-3].

The electronic structure of novel type of organic conductors, ammonium tetrathiafulvalene carboxylate (TTFCOO) and its and tetrathiapentalene derivative (TTPCOO) was investigated by high-field ESR and NMR measurements. The pristine TTFCOOH and TTPCOOH molecules are closed-shell. Kobayashi and coworkers found that self-doped type carrier was generated by substitution of the end group of (NH_3^0) with (NH_4^{+1}), which is regarded as a charge-reservoir. They developed a variety of self-doped organic conductor families. Because of sample limitation (powder), the detailed electronic state (anisotropic *g*-tenor and linewidth) was not clarified within the framework of conventional X-band ESR spectroscopy. In order to investigate the electronic structure from the microscopic point of view, we use the high-field W-band (94GHz) ESR spectrometer. By using W-band, a clear powder pattern structure could be found. We can evaluate the principal values of the *g*-tensor for theses salts, assuming anisotropic *g*-values. We found that TTFCOO system shows 1D column structure. On the other hand, the TTPCOO derivative system seems to be isotropic structure within 2D layer. As a result, TTFCOO system is a narrow-gap semiconductor because of 1D instability, while TTPCOO shows a stable metallic state down to 2K. Detailed discussion including ^{1}H-NMR results is presented.

MurD is one of the ATP-driven Muramyl ligases that are responsible for peptidoglycan biosynthesis. The crystal structures of MurD indicate that one of the three domains of MurD, domain 3, undergoes drastic conformational change from open to closed state, which controls the process of the reaction. However the detailed mechanism of its regulation has not been clarified. How the binding of the ligands triggers the open-close transition of domain 3 is an open question. To investigate the dynamic structural changes of domain 3 coupled with the enzymatic process, Hokkaido Univ. group exploited paramagnetic lanthanide probe, where paramagnetic lanthanide ion is fixed in a protein frame. ESR is advantageous because we can get long-distance information and high sensitivity. To understand the steric structure and mechanism of function especially for MurD, we investigate the MurD tagged Gd^{3+} ligand by ESR spectroscopy. Detailed experimental results will be presented in this symposium.

These investigations are joint researches with Dr. M. Asada (IMS), Prof. K. Furukawa (Present address: Niigata Univ.), Mr. S. Hiramatsu, Dr. T. Saio, Prof. K. Ishimori (Hokkaido Univ.).

[1] K. Furukawa, T. Nakamura, Y. Kobayashi and T. Ogura, J. Phys. Soc. Jpn., 79 (2010) 053701.
[2] K. Furukawa, T. Hara, and T. Nakamura, J. Phys. Soc. Jpn. 2010, 79, 043702 (4 pages).
[3] K. Furukawa, Y. Sugishima, H. Fujiwara and T. Nakamura, Chem. Lett. 2011, 40 292-294.
[4] S. Jin, M. Supur, M. Addicoat, K. Furukawa, L. Chen, T. Nakamura, S. Fukuzumi, S. Irle, D. Jiang, J. Am. Chem. Soc. 137 (2015) 7817–7827, and references therein.
[5] T. Nakamura, K. Furukawa, T. Terauchi, and Y. Kobayashi, Phys. Status Solidi RRL 9 (2015) 480–484.

Geometry and electron tunneling route of photoinduced primary charge-separated state in the photosynthetic reaction center

M. Hasegawa[1], H. Nagashima[2], R. Minobe[1], T. Sakai[2], T. Tachikawa[1], H. Mino[2] and
Y. Kobori[1]

[1]*Graduate School of Science, Kobe University, Kobe 657-8501, Japan.*
[2] *Graduate School of Science, Nagoya University, Nagoya 464-8602, Japan.*

Email: ykobori@kitty.kobe-u.ac.jp

In initial events of the photosynthesis by higher plants, the photosystem II (PSII) generates photoinduced primary charge–separated (CS) state composed of reduced pheophytin ($\mathrm{Pheo}_{D1}^{-\bullet}$) and oxidized special pair ($P^{+\bullet}$) in chlorophylls a (Chla) P_{D1}/P_{D2} in the D1/D2 heterodimer, ultimately leading to the water oxidation at the oxygen–evolving Mn_4CaO_5 cluster by $P^{+\bullet}$ (Fig. 1). Several studies have been performed to understand mechanisms of an extremely high redox potential of $P^{+\bullet}$ in PSII while the photosynthetic reaction centers (PRC)[1] do not have such potentials in purple bacteria.[2,3] It has been suggested that the cationic charge localization of the D1 part (P_{D1}) at 70-80 % over P_{D1}/P_{D2} may lower the singly occupied molecular orbital (SOMO) level and play a role on the exothermic Mn_4CaO_5 oxidization.[2,3] However no experimental studies have been performed to identify charge locations, molecular conformations, and electronic interaction in the primary CS state in which the anionic charge of $\mathrm{Pheo}_{D1}^{-\bullet}$ may significantly influence the electronic state in the PSII RC. In particular, Pheo_{D1} employs a vinyl group as a terminal substituent which is located in close proximity to Chl_{D1} as shown in Fig. 1, whereas the bacterial pheophytin (H_A) utilizes an acetyl group as one of the electron-tunneling routes between the accessory chlorophyll (B_A) and H_A.[4] It has been unclear how the vinyl substituent plays a role on the electronic couplings for the initial light-energy conversion.

To understand molecular mechanism of the efficient generation of the initial oxidative state, we have characterized geometries and orientations of the photoinduced CS states in the PRC from *Rhodobacter sphaeroides*[1] and in the PSII from spinach using the X-band time-resolved EPR (TREPR)[1,5-7] method. In the spinach, we have obtained the TREPR spectra of the primary CS states in quinone pre-reduced membranes of PSII in frozen solution and in oriented multilayers at 77 K. It has been revealed that the cationic charge is localized in P_{D1} of the special pair at a close distance of 1.5 nm from $\mathrm{Pheo}_{D1}^{-\bullet}$ but that the electronic coupling between the charges is significantly weak owing to the vinyl substituent, resulting in the long-lived CS state generation in the PSII.

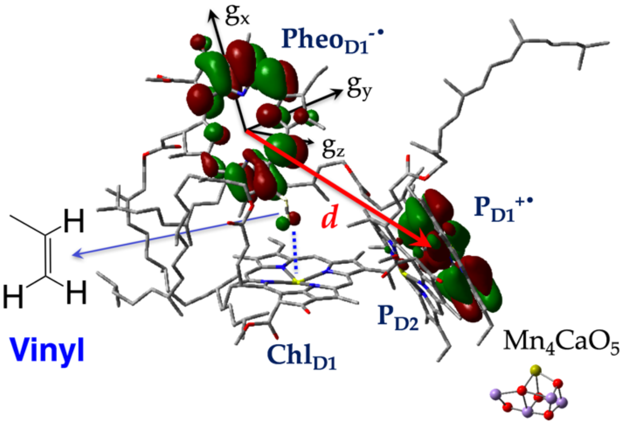

Fig. 1: Geometry of the photoinduced primary CS state in the PSII reaction center

(1) Kobori, Y.; Ponomarenko, N.; Norris, J. R. *J. Phys. Chem. C* **2015**, *119*, 8078-8088.
(2) Okubo, T.; Tomo, T.; Sugiura, M.; Noguchi, T. *Biochemistry* **2007**, *46*, 4390-4397.
(3) Saito, K.; Ishida, T.; Sugiura, M.; Kawakami, K.; Umena, Y.; Kamiya, N.; Shen, J.-R.; Ishikita, H. *J. Am. Chem. Soc.* **2011**, *133*, 14379-14388.
(4) O'Malley, P. J. *J. Phys. Chem. B* **2000**, *104*, 2176-2182.
(5) Miura, T.; Tao, R.; Shibata, S.; Umeyama, T.; Tachikawa, T.; Imahori, H.; Kobori, Y. *J. Am. Chem. Soc.* **2016**, *138*, 5879-5885.
(6) Kobori, Y.; Miura, T. *J. Phys. Chem. Lett.* **2015**, *6*, 113-123.
(7) Kobori, Y.; Noji, R.; Tsuganezawa, S. *J. Phys. Chem. C* **2013**, *117*, 1589-1599.

T-3

Converting NMR signals into light via a membrane capacitor

Kazuyuki Takeda[1]

[1]*Graduate School of Science, Kyoto University, Kyoto 606-8502, Japan.*

Email: takezo@kuchem.kyoto-u.ac.jp

To open the possibility of sensitive NMR measurement, we explore an unprecedented experimental approach, in which radiofrequency signals are up-converted to optical carriers[1] using a capacitor made of an elastic, high-Q SiN membrane.

In such a capacitor, displacement of the membrane changes the capacitance, thereby affecting the resonant mode of the probe circuit. Conversely, electric charges on the electrodes of the capacitor cause the Coulomb force that pulls the membrane. Thus, electromotive force due to nuclear-spin induction is converted to the membrane displacement, which can be read out by an optical interferometer. Since optical measurements can be performed with quantum-limited accuracy, the sensitivity of the NMR signal detected in this way is expected to be very high, provided that both thermal noise in the resonant circuit and thermal fluctuation of the membrane are suppressed. Here, we report our recent development of such an *opto-electro-mechanical NMR* system (Fig. 1).

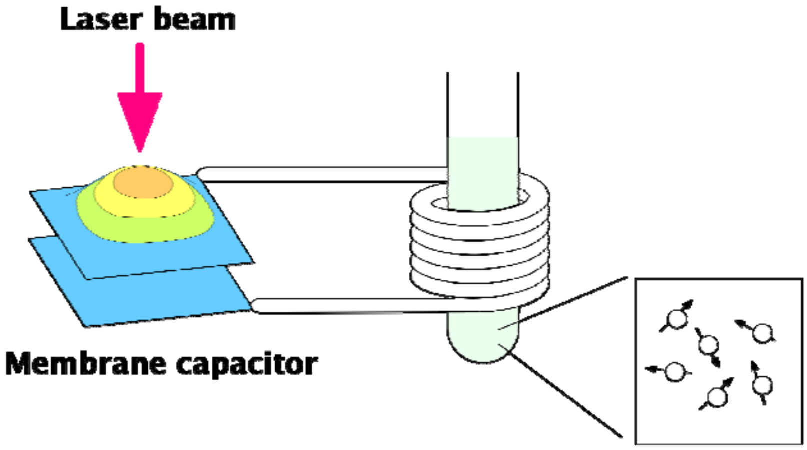

Fig. 1. Schematic description of opto-electro-mechanical NMR.
Nuclear induction develops the electromotive force in the tuned circuit, which, in turn, causes displacement of the membrane of the capacitor. The NMR signal originally appearing as an radiofrequency signal is eventually transferred to an optical carrier.

[1] T. Bagci, A. Simonsen, S. Schmid, L. G. Villanueva, E. Zeuthen, J. Appel, J. M. Taylor, A. Sørensen, K. Usami, A. Schliesser, E. S. Polzik, Nature **507**, 81-85 (2014).

T-4

Magnetic resonance force measurements by high sensitive Si cantilever with a magnet particle

Masaya Toda

Graduate School of Engineering, Tohoku University, Sendai 980-8579, Japan.

Email: mtoda@nme.mech.tohoku.ac.jp

Our laboratory is focusing on the detection of biological information of living cells using electron spin resonance detection. Our recent trials will be presented in this talk (Fig. 1).

The magnetic resonance force microscopy (MRFM) is a good possibility to image the inside of a bio-cell. Currently the measurement time and resolution are the issues. To make the measurement time shorter and the resolution higher the detectable force and response time should be as small as possible. Based on the force noise level, the force sensor should be narrow, thin and long enough such as a nanowire structure. In our previous research, we developed a 210 nm-wide and 32 μm-long silicon nanowire probe with a silicon mirror using a silicon-on-insulator wafer in order to improve sensitivity of force detection for MRFM. A NdFeB magnet was integrated at the end of the nanowire. The detected force and magnetic field gradient are approximately 82 aN and ~70.1 G μm^{-1} at room temperature. The radical density is calculated as 4.6 × 10^{18} spins per cm^{-3}[1].

The living cell is in liquid, which is not the situation which gives the best performance for the force sensor. It means that the target sample should be in liquid of atmospheric pressure and the force sensor should be in an ultrahigh vacuum. One possibility is the use of microchannel with a thin window [2]. A micro fluidic chamber with single crystal Si windows of 178 nm-thick on a micro channel has been developed. Because of these thin windows, the aquatic structure inside of the channel can be observed by scanning electron microscopy. Secondary electrons from the sample in the channel are able to be detected in vacuum with the acceleration voltage of 15 kV. The micro fluidic chamber is possibly applied to cell imaging via the Si thin window in vacuum using magnetic resonance force microscopy. The other possibility is a packaging of the force sensor. The packaging techniques of a cantilever by Al-Al direct metal bonding method and anodic bonding technique under high vacuum condition to fabricate packaging device with vacuum condition have been demonstrated. The purpose of this study is to fabricate a packaged cantilever for magnetic force sensing that can be used under atmospheric pressure.

To reduce the thermal noise, the temperature need to be extremely decreased. However the performance of scanner, ex. piezoelectric actuator, is decreased at the low temperature. To keep the long stroke distance of the scanner, the 3D scanner based on electrostatic force has been developed.

Not only imaging method, the magnetic resonance force detection can be used as a part of flow cytometry. Jurkat cells incubated to 10^5-10^6 concentration is used to evaluate fluidic, electrical, and mechanical function of the device. The measurement example by a standard flow cytometry will be introduced. Combing the magnetic resonant force measurement, the concentrations of the active oxygen in flowing cell in micro channel will be measured without any levels.

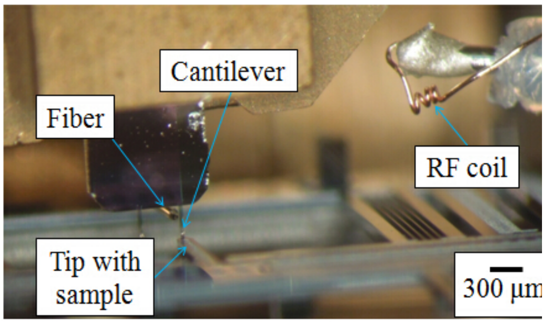

Fig. 1: MRFM set-up in Tohoku University.

[1] Y.-J. Seo, M. Toda, T. Ono, *J Micromech Microeng* **2015**, *25*, 045015.

[2] H. Hayashi, M. Toda, T. Ono, Proceedings of the *IEEE International Conference on Micro Electro Mechanical Systems,* **2015**, 344.

[3] G. Xue, M. Toda, T. Ono, *IEEJ Transactions on Sensors and Micromachines* **2015**, *135*, 236.

Development and application of force-detected THz-ESR measurement system

H. Takahashi[1], T. Okamoto[2], E. Ohmichi,[2] and H. Ohta[3]

[1]Organization for Advanced and Integrated Research, Kobe University, Kobe 657-8501, Japan.
[2]Graduate School of Science, Kobe University, Kobe 657-8501, Japan.
[3]Molecular Photoscience Research Center, Kobe University, Kobe 657-8501, Japan.

Email: hide.takahashi@crystal.kobe-u.ac.jp

In mechanically-detected ESR measurements, ESR is detected as a cantilever displacement induced by the change in the sample magnetization. This technique has some advantages over conventional methods which measure the microwave power absorbed by a sample. The most important feature is that it can measure a tiny sample because of high force sensitivity. The sample mass mounted on the cantilever is on the order of ng-ug. We expect that this feature is suitable for the study of biological materials such as metalloproteins. ESR is generally a powerful technique to study biological materials because it directly probes the metal ion sites that play an important role in the emergence of functionality. Since the sample preparation process of biological matters is time-consuming, cantilever technique that requires only ng mass saves on cost and time, and improves the measurement throughput.

In the application of the biological materials, it is also of great advantage that cantilever technique can be used between very broad frequency ranges (GHz-THz) without changing the most part of experimental setup. It can observe the ESR signal across large zero-field splitting that cannot be observed by a commercial X-band spectrometer.

Last year, we for the first time reported the mechanical detection of ESR signals beyond 1 THz by using the combination of piezoresistive cantilever and backward wave oscillators [1]. However, the spin sensitivity that we achieved in this measurement was not sufficient for the measurement of metalloproteins that have very low spin density. For further sensitivity improvement, now we are developing the measurement system based on the optical interferometric detection [2, 3]. In our new system, the wavelength tunable laser source (wavelength is 1465-1575 nm) is used for the feedback-control of interferometer tuning. Such tuning control is crucial to resolve several issues such as sensitivity fluctuation and self-oscillation induced by photothermal effect. Using this system, we successfully observed ESR signals from 16 ng sample of Hemin in the frequencies of up to 0.5 THz. The spin sensitivity is no worse than 10^9 spin/gauss at 130 GHz, which was improved by more than two orders of magnitude compared to our previous result using piezoresistive detection [4]. We believe that the metallprotein measurement will be possible in the near future.

This research was partly supported by a Grant-in-Aid for Young Scientists (B) (16K17749), Grants-in-Aid for Scientific Research (B) (Nos.22340101 and 26287081) and by a Grant-in-Aid for Challenging Exploratory Research (No. 26610104) from JSPS, and by the Asahi Glass Foundation.

[1] H. Takahashi, E. Ohmichi and H. Ohta, Appl. Phys. Lett. **107**, 182405 (2015).
[2] E. Ohmichi, Y. Tokuda, R. Tabuse, D. Tsubokura, T. Okamoto and H. Ohta, Rev. Sci. Instrum. **87**, 073904 (2016)
[3] H. Takahashi, T. Okamoto, E. Ohmichi and H. Ohta, Appl. Phys. Express **9**, 126701 (2016).
[4] E. Ohmichi, T. Okamoto, M. Mitani, H. Takahashi, H. Ohta, J. Inorg. Biochem, in press.

T-6

Development of CW-EPR-based oxygen mapping using dicarboxy-PROXYLs and single-point imaging modality

H. Hirata

Graduate School of Information Science and Technology, Hokkaido University, Sapporo 060-0814, Japan.

Email: hhirata@ist.hokudai.ac.jp

In this talk, the concept of simultaneous imaging of oxygen partial pressure pO_2 and nitroxyl radical concentration using isotopic nitrogen labeling is presented. Since the concentration of a spin probe affects its EPR linewidth (or the relaxation time T2), measurements of pO_2 have traditionally required simultaneous estimation of the probe concentration. Methods for measuring pO_2 using monohydrogenated CTPO (mHCTPO) were developed in the 1990s to overcome this dependence on the concentration of the probe [1–3]. That approach requires spectral-spatial EPR imaging to obtain spectral information and pO_2 maps. In order to avoid the technical difficulties in spectral-spatial imaigng, single-point imaging (SPI) modality [4,5] was used for relaxation measurements of probes in this study. To simultaneously measure unknown parameters (pO_2 and the concentrations of the probes), a pair of isotopic nitroxyl radicals, such as ^{14}N- and ^{15}N-labeled dicarboxy-PROXYLs (^{14}N-DCP and ^{15}N-DCP) were used as oxygen-sensitive spin probes (DCP probes were synthesized by Dr. I. A. Kirilyuk at Novosibirsk Institute of Organic Chemistry) [6]. First, simultaneous equations for expressing the effects of the self-broadening of ^{14}N- and ^{15}N-DCPs, cross-broadening between ^{14}N- and ^{15}N-DCPs, and oxygen-broadening on the linewidths of the probes were established. Linewidth maps could be obtained from T2* maps measured from a mixture of ^{14}N- and ^{15}N-DCPs. The concentrations of the probes and pO_2 could then be calculated simultaneously by solving the simultaneous equations.

This work was supported by JSPS KAKENHI grant number 26249057 and 16K12862.

[1] H. J. Halpern *et al*., *J. Magn. Reson*., **1990**, *90*, 40–51.
[2] H. J. Halpern *et al*., *J. Magn. Reson*., **1993**, *A103*, 13–32.
[3] H. J. Halpern *et al*., *Proc. Natl. Acad. Sci. USA*, **1994**, *91*, 13047–13051.
[4] S. Subramanian *et al*.. *Magn. Reson. Med*., **2002**, *48*, 370–379.
[5] K. Matsumoto *et al*., *Magn. Reson. Med*., **2003**, *50*, 865–874.
[6] A. A. Gorodetsky *et al*., *Magn. Reson. Med*., **2016**, *76*, 350–358.

T-7

Development of DNP-MRI scanners at wide frequency range for biomedical application -from skin to large animal-

K.Ichikawa

Innovation Center for Medical Redox Navigation, Kyushu University, Fukuoka 812-8582, Japan.

Email: ichikawa.kazuhiro.684@m.kyushu-u.ac.jp

Free radical compounds are sensitive to their surrounding environment and have been used as molecular probe of biophysical parameters. A class of aminoxyl (nitroxyl) radicals has been frequently used for detecting reduction-oxidation (redox) status, pH or partial oxygen pressure in vivo, based on its free radical status, absorption lineshape. The spatial resolution of the radical distribution detected by ESR technique is in the range of few to dozen mm and is difficult to be compared with corresponding organ structure.

Dynamic nuclear polarization (DNP) is one of spin polarization techniques based on different spin-spin system. Electron spin has been utilized to hyperpolarize proton spin to transfer "electron information" to MRI, achieving free radical image in high spatial resolution. For in vivo observation, external magnetic field of DNP-MRI is frequently in the range of 0.005 to 0.01 Tesla, to ensure good microwave penetration into animal and the S/N ratio is limited.

We have been developing DNP-MRI scanners at different frequency ranges to maximize S/N ratio of the DNP-MRI system for target tissues from skin to large animal (Fig 1a). One end of our R&D is DNP-MRI system for pig measurement, whose specifications are: main magnet 0.01 Tesla; gap size 350mm; homogenous volume 250mm, with 165mm DNP-MRI resonator; resonant frequencies and Q values of 404kHz/180, 267-280MHz/160 for NMR and ESR, respectively. Other end of the R&D is a 0.15 Tesla DNP-MRI system for skin measurement, whose specifications are: main magnet 0.15 Tesla permanent magnet; gap size 160 mm; homogenous volume 80 mm, with TE_{101} cavity mode DNP-MRI resonator; resonant frequencies and Q values of 6.38MHz/150, 4.31-4.41GHz/120 for NMR and ESR, respectively.

The MRI S/N ratio of 0.15 Tesla DNP-MRI system was improved by factor of 50 compared with low frequency DNP-MRI and phantom object were clearly resolved, suitable for skin measurement in high resolution (Fig 1b right). The designs and performances of our DNP-MRI systems will be shown in in the presentation.

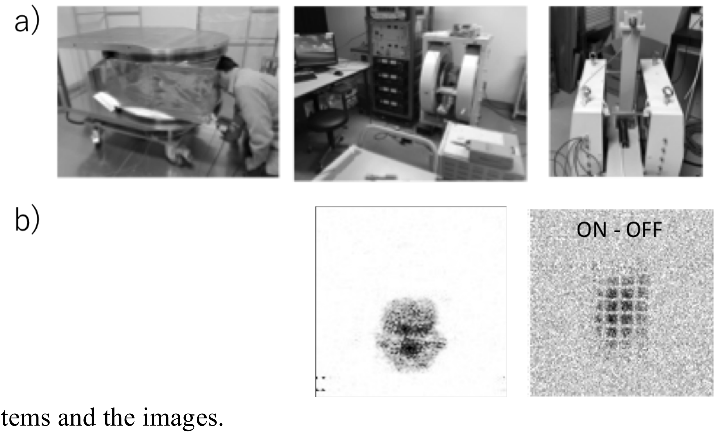

Fig. 1: DNP-MRI systems and the images.
a) 0.01, 0.04 and 0.15 Tesla DNP-MRI systems (left to right) b) MC-PROXYL radical distribution images at mouse brain (left, FOV=48x48mm, voxel size =0.5x0.5x3mm) and phantom images of carboxy PROXYL (right, FOV=64x64mm, 0.5x0.5x2mm)

T-8

Dynamic nuclear polarization with double 460 GHz gyrotrons for the sensitivity enhancement of magic-angle-spinning NMR at 30 K

T. Fujiwara and Y. Matsuki

Institute for Protein Research, Osaka University, Suita 565-0871, Japan.

Email: tfjwr@protein.osaka-u.ac.jp

NMR sensitivity is the crucial factor for studying the structures of large biomolecules. We are improving the instrumentation for high-field dynamic nuclear polarization (DNP) to increase the sensitivity of high-resolution solid-state ^{13}C NMR. Our previous experiments showed that DNP at about 30 K provided much higher polarization than those at about 90 K. At first, these magic-angle-spinning (MAS) DNP experiments were performed by boiling liquid helium. Thus the large liquid He consumption made the routine DNP experiments difficult. To minimize the He consumption, we have developed a closed He-gas circulation system with an electrical gas chiller for MAS experiments at about 30 K. This circulation system not only reduced the operation cost but also stabilized the gas flow over an experimental time of a week for multidimensional NMR experiments. The large Boltzmann polarization and reduced thermal noise at the low temperature increased the NMR sensitivity. We developed a high-power submillimeter wave irradiation system with two gyrotrons to saturate electron spin resonances of paramagnetic compounds efficiently at 16.4 T. One second-harmonics gyrotron generates a high-intensity 460-GHz wave with a continuously tunable range of about 1 GHz. The other gyrotron provides the submillimeter wave with frequency modulation at the rate about 10 kHz. The submillimeter waves are transmitted to a sample rotor through a diplexer connected to corrugated waveguides. This system was used for double resonance experiments in a submillimeter wave range which should improve the high-field DNP experiments. We will present the experimental results obtained with our DNP-NMR spectrometer.

Instrumentation for DNP was developed with Research Center for Far-Infrared Region in Fukui University and JEOL RESONANCE Ltd. under the support by JST Sentan and NMR platform, Japan.

[1] Y. Matsuki, T. Idehara, J. Fukazawa, and T. Fujiwara. Advanced instrumentation for DNP-enhanced MAS NMR for higher magnetic fields and lower temperatures, J. Magn. Reson., **264** (2016) 107.

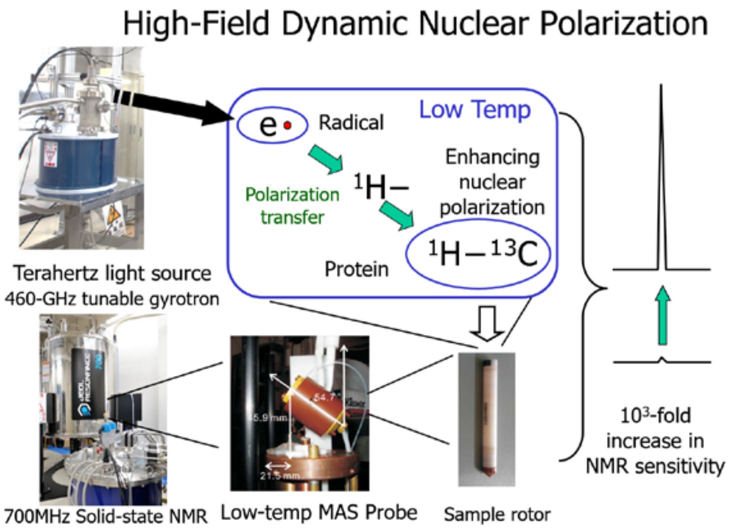

Fig. 1: Instrumentation for high-field DNP NMR.

Application of distance determination using spin labeling dipolar EPR spectroscopy to complex protein system: 3-dimensional organization and regulatory action of troponin-tropomyosin in muscle thin filament

T. Arata,[1] K. Ueda,[1] C. Zhao,[1] K. Sakai,[1] H. Yamashita,[1] Y.Tujimoto,[1] S. Ueki,[2] and M. Miki[3]

[1]*Graduate School of Science, Osaka University, Osaka 560-0043, Japan.*

[2]*Kagawa School of Pharmaceutical Sciences, Tokushima Bunri University, Kagawa 769-2193, Japan.*

[3]*Graduate School of Engineering Science, University of Fukui, Fukui 910-8507, Japan.*

Email: arata@bio.sci.osaka-u.ac.jp

CW [1] and pulse dipolar EPR, PELDOR or DEER [2] and DQC [3], can determine a distribution of the distance 0.8-8.0 nm between two spin labels attached to protein by site-directed genetic mutagenesis (SDSL-EPR). Muscle contraction is triggered by Ca^{2+}. Heart muscle beating is further regulated (fine-tuned) by phosphorylation of cardiac troponin I (cTnI). We have determined the secondary structure of N-terminal phosphorylatable extension of cTnI, intrinsically disordered protein (IDP) region invisible in the crystal structure, by measuring the distance distribution between two spin labels attached on *i* and *i+4* residues [4]. Most of the CW-EPR spectra of these regions showed a broad residual distance distribution over 0.8-2.0 nm, suggesting a largely disordered structure. However, 23/27 and 43/47, located at PKA and PKC phosphorylation sites, showed narrow distance distributions in the cTnI-cTnC complex than in the monomer. This suggests that only two phosphorylation sites of cTnI interact 'stereospecifically' with cTnC to maintain high Ca^{2+} affinity state and that they release from cTnC upon phosphorylation to produce low affinity state.

We have also applied this technique to a large protein assembly of giga-dalton molecular weight. Troponin (Tn)-tropomyosin (Tm) in the thin filament of microns in length blocks or allows myosin binding to actin in response to Ca^{2+}. First, we targeted the functionally important region of TnI subunit, the regulatory switch, and used pulse EPR to obtain the positioning of this region with and without Ca^{2+}[5]. The interspin distance between TnC and TnI revealed a large 5 nm movement, *i.e.,* complete release and close proximity in the absence and presence of Ca^{2+}, respectively. This movement is sufficient for translocation of Tm from blocked to open state. Then, we next determined the position of Tm (rod-like head-to-tail N-C jointed polymers) in the thin filament with and without Ca^{2+}. By using CW-EPR we examined the thin filament reconstituted from various ^{15}N-based spin labeled residues of Tm and ^{14}N-based spin labeled actin. Distance distribution was obtained by analyzing dipolar interaction in the difference spectrum where non-interacting ^{14}N spectrum was subtracted out using distinct spectral characteristics of ^{14}N- and ^{15}N-labels. Ca^{2+} effects on the distance were found but restricted only at the N- and C-terminal region of Tm-Tm junction. Distance between spin labeled Tm and actin (Mn^{2+}-ADP) were also determined to be 2-2.5 nm at some residues but beyond sensitivity (>2.5 nm) at the other over a wide region of Tm. We are constructing the model of Tm positioning on actin filament by mapping with several sets of Tm-actin distances. A preliminary model showed a small Ca^{2+}-induced movement (<0.5 nm) of Tm along the thin filament and flared structure at the N-C junction without Ca^{2+}. Flexibility of Tm at the junction was also suggested by the fact that the interspin distance between Tm and cTnT at the junction was heterogeneous and included the populations with the distance much longer than as well as close to that of the fragmented Tm-TnT crystal (PDB:2Z5H).

[1] S. Ueki, M. Nakamura, T. Komori, and T. Arata, Biochemistry **44** (2005) 411.
[2] M. Nakamura, S. Ueki, H. Hara, and T. Arata, J. Mol. Biol. **348** (2005) 127.
[3] J.Abe, S.Ueki, T.Arata, S.Nakazawa, S.Yamauchi, and Y.Ohba, Appl. Mag. Reson. **42** (2012) 273.
[4] C.Zhao, Y.Somiya, S.Takai, S.Ueki, T.Arata, Biophys.J.**102** (2012) 406a; Sci. Rep. in press(2016).
[5] T.Aihara, M. Nakamura, S.Ueki, H. Hara, M.Miki, and T. Arata, J. Biol. Chem. **285** (2010) 10671.
[6]K.Ueda,C.Kimura-Sakiyama,T.Aihara,M.Miki,T.Arata, Biophys.J.**100**(2011) 2432;**105**(2013)2366.

T-10

Local structure of photosystem II revealed by pulsed ELDOR

Hiroyuki Mino[2]

[1]Graduate School of Science, Nagoya University Furo-cho, Chikusa, Nagoya, 464-8602, Japan

E-mail: mino@bio.phys.nagoya-u.ac.jp

X-ray crystallography provides the detail structural information of the protein, giving the important clues to understand enzyme function [1]. However, the obtained structure is static and function is not derived directly. Various EPR techniques enable to determine the distances between radicals in the proteins, giving the protein-protein interactions and the insight of the function. Photosystem (PS) II protein complex is a catalyst of the photosynthetic oxygen evolution. We will present the recent results about PS II.

The Mn cluster consists of four Mn and one Ca ions. Assembly of the Mn cluster is initiated by visible light in the presence of Mn and Ca ions. This process is called as “photoactivation”, which has been studied using OEC-removed PS II membranes. The initial reaction of photoactivation is proposed to be incorporation of one Mn^{2+} to a high-affinity site of apo-PS II in dark state, called IM$_0$ state. In the initial IM0 state, there is one specific binding site of Mn^{2+} that is photo-oxidized to Mn^{3+}. We measured a distance between a redox-active tyrosine residue $Y_D^{\bullet}$ and the Mn^{2+} binding to the high-affinity site by PELDOR. The distance between $Y_D^{\bullet}$ and Mn^{2+} was estimated to be 30.5 ± 0.5 Å. By calculating with the coordinates of possible positions, the high-affinity site is indicated to be located at the position of the Mn4 in the active manganese cluster.

The main reaction center of PS II is well conserved in species, however, the extrinsic subunits have variety depending on the species. PsbP is an extrinsic subunit of PS II in higher plants and maintains oxygen-evolving activity of PS II. The molecular structure of PS II isolated from cyanobacteria has been revealed by recent X-ray structural analysis, however, the binding site and topology of PsbP in PS II are still unknown. In this study, the location of the PsbP in PS II complex was revealed by pulsed electron-electron double resonance (PELDOR).

MSL spin labels were introduced to the four residues of the Cys-introduced PsbP mutants. Each MSL-labeled PsbP mutant was reconstituted to a PS II whose extrinsic subunits had been depleted in pretreatment. We measured the distances between Y_D• and MSL-labeled moieties of PsbP by PELDOR. The distance between Y_D• and the center of PsbP was calculated as 45.5 Å based on the PELDOR results, and is similar to the distance of 46.5 Å between the Y_D• and the center of PsbV of cyanobacteria obtained from the crystal structure [1]. The topological information was consistent with the mobility of the spin labels at the Cys-introduced sites in PsbPs obtained by CW-EPR spectroscopy. The interaction between PsbP and the oxygen evolving complex will be discussed.

References

[1] Suga M. et al., Nature, 2015, 517, 99-103.
[2] Nishimura T. et al., Biochim. Biophys. Acta, 2014, 1837, 1447-1453

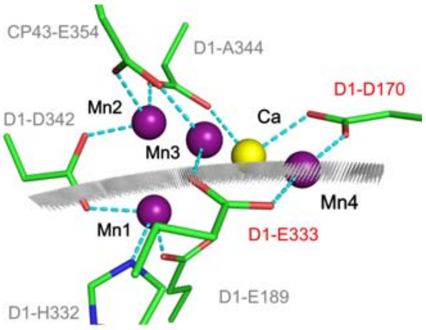

Fig1: the location of the Mn^{2+} affinity site determined by PELDOR

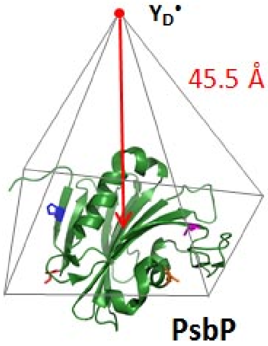

Fig2: the location of the PsbP-protein determined by PELDOR.

T-11

ENDOR reveals how radical SAM enzymes tame highly reactive radical

M. Horitani,[1] K. Shisler,[2] W. E. Broderick,[2] R. U. Hatcheson,[2] K. S. Duschene,[2] A. R. Marts,[1]
B. M. Hoffman,[1] and J. B. Broderick[2]

[1]*Department of Chemistry, Northwestern University, Evanston 60208, USA.*

[2]*Department of Chemistry & Biochemistry, Montana State University, Bozeman 59717, USA.*

Email: m-horitani@northwestern.edu

Radical SAM (*S*-adenosylmethionine) enzyme is the largest known enzyme super family with more than 100,000 functional domain found throughout all kingdoms of life. All enzyme has unique [4Fe-4S] cluster and catalyze a diverse array of finely tuned radical reaction by using 5'-deoxyadenosyl (5'-dAdo•) radical which is generated from the reductive cleavage of SAM. Previously, our electron nuclear double resonance (ENDOR) studies revealed that unique iron ion is coordinated with amino and carboxyl moiety of methionine in SAM [1], subsequently X-ray crystallographic studies confirmed this. To date, neither 5'-dAdo• radical nor SAM- or 5'-dAdo-derived intermediate have been trapped and observed for not only any radical SAM enzyme but vitamin B_{12} coenzyme, which also utilize same 5'-dAdo• radical generated from adenosylcobalamin.

Pyruvate formate-lyase activating enzyme (PFL-AE) is a member of radical SAM enzyme that catalyzes the formation of glycyl (G•) radical on G734 of PFL. We try to use rapid freeze-quench (rfq) technique, electron paramagnetic resonance (EPR) and ENDOR spectroscopies to trap and characterize the catalytically competent intermediate species formed by the PFL-AE catalytic reaction. When the photoreduced PFL-AE is mixed and rapidly quenched with PFL and SAM by rfq of time range of 25 ms to 1 s, the characteristic $[4Fe\text{-}4S]^+$ EPR signal is diminished and a new EPR signal (denoted Ω) is appeared, whose intensity is reached a maximum at 500 ms quenching time. During cryo-annealing, the Ω signal is lost in parallel with quantitative generation of G• radical. This confirms that the Ω is the catalytically competent intermediate. To further characteristic studies, we perform the rfq ENDOR measurements for ^{13}C labeled SAM and ^{57}Fe labeled PFL-AE. ENDOR results reveal that the Ω is unexpectedly an organometallic compound which 5'C of 5'-dAdo covalently binds with [4Fe-4S] cluster [2]. This discovery extends the list of organometallic centers to the radical SAM enzymes and reveals intriguing parallels to B_{12} radical enzymes.

Moreover, we try to trap and characterize 5'-dAdo• radical analogue intermediate in lysine 2,3-aminomutase, which is also a member of radical SAM enzyme, by use of SAM analogue, anSAM (3',4'-anhydro-*S*-adenosylmethionine) [3]. In this workshop, I will present all intermediate characterizations and proposed overall reaction mechanism of radical SAM enzyme (Fig. 1).

[1] C. J. Walsby, D. Ortillo, W. E. Broderick, J. B. Broderick, and B. M. Hoffman, J. Amer. Chem. Soc.**124** (2002) 11270.

[2] M. Horitani, K. Shisler, W. E. Broderick, R. U. Hatcheson, K. S. Duschene, A. R. Marts, B. M. Hoffman, and J. B. Broderick, Science **352** (2016) 822.

[3] M. Horitani, A. S. Byer, K. A. Shisler, T. Chandra, J. B. Broderick, and B. M. Hoffman, J. Amer. Chem. Soc. **137** (2015) 7111

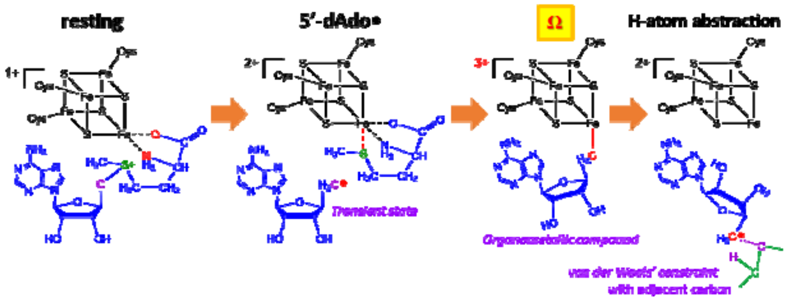

Fig. 1: Proposed reaction mechanism of radical SAM enzymes

Novel possibilities in solid state NMR: cryoMAS down to 10 K and NMR in pulsed magnetic fields up to 70 T.

Ivo Heinmaa,[1] Hannes Kühne,[2] and Raivo Stern [1,2,3]

[1] National Institute of Chemical Physics and Biophysics, Tallinn 12618, Estonia.

[2] Dresden High Magnetic Field Laboratory (HLD-EMFL), Dresden 01314, Germany.

[3] Division of Materials Physics, Grad. School of Eng. Science, Osaka University, Toyonaka 560-8531, Japan.

Email: raivo.stern@kbfi.ee; raivo.stern@gmail.com.

The T < 77 K MAS NMR (cryoMAS) [1] is an important prequisite for DNP applications in biological samples. We have developed a cryoMAS design allowing us to work down to 10 K with still 10 kHz spinning and demonstrate this approach on various solid state examples [2] (Fig. 1, Left).

We also have performed ^{11}B NMR on $SrCu_2(BO_3)_2$ in pulsed magnetic fields up to 70 T resulting in a very good agreement with a transition from a high-temperature, paramagnetic state to a low-T, commensurate superstructure of field-induced spin-dimer triplets in the 1/3 magnetization plateau. The technical approach to measure broadband NMR in pulsed fields was developed in the course of this work, opening the door to studies of many other materials (incl.quantum magnets) with complex interactions that stabilize new phases of matter in very strong magnetic fields [3] (Fig. 1, Right).

[1] A. Samoson, T. Tuherm, J. Past, A. Reinhold, T. Anupõld, I. Heinmaa. New Horizons for Magic-Angle Spinning NMR. In: Topics in Current Chemistry (15−31). Springer Verlag, (2004).
[2] R. Stern, I. Heinmaa, E. Joon, A.A. Tsirlin, H. Nakamura, T. Kimura. Appl. Mag. Res. **45**, 1253 (2014).
[3] J. Kohlrautz, J. Haase, E.L. Green, Z.T. Zhang, J. Wosnitza, T. Herrmannsdörfer, H.A. Dabkowska, B.D. Gaulin, R. Stern, and H. Kühne. J. Magn. Reson. **271**, 52 (2016).

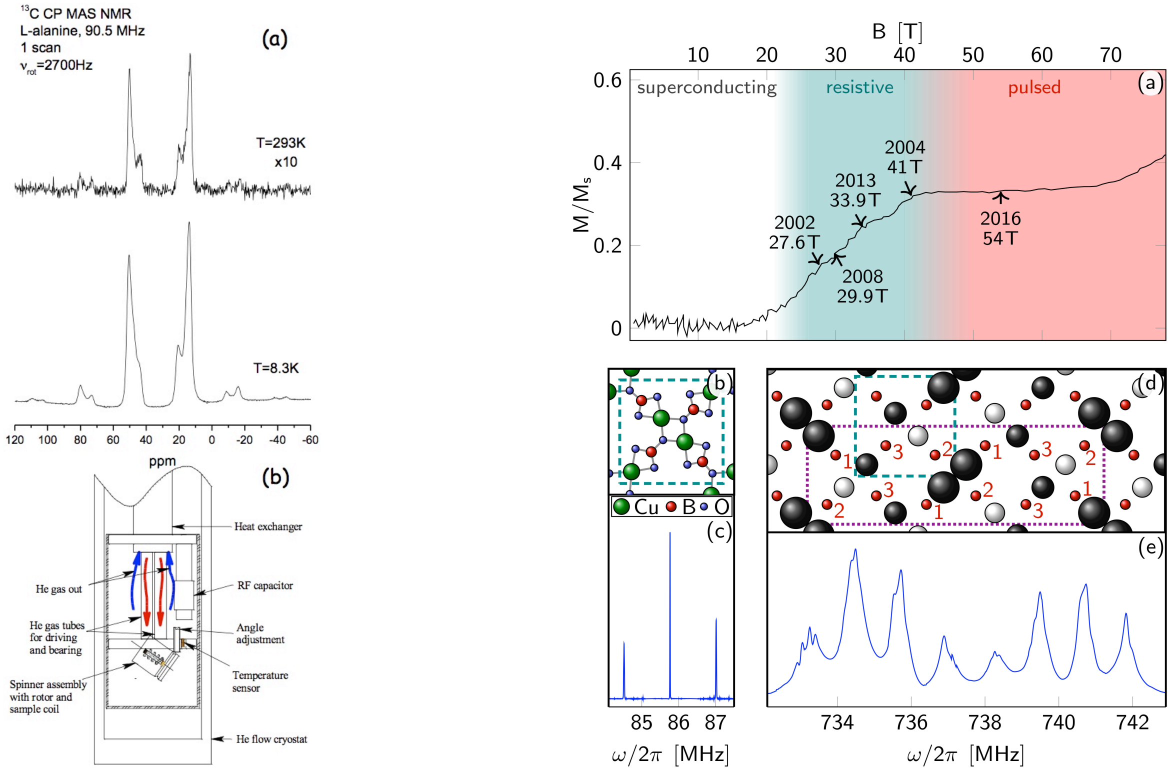

Fig. 1: **Left:** (a) L-alanine cryoMAS spectra at 293 K and 8.3 K. (b) Schema of our cryoMAS. **Right:** (a) Macroscopic magnetization of $SrCu_2(BO_3)_2$ at 2 K (from Matsuda *et al.* Phys. Rev. Lett. **111** (2013) 137204). (b) Unit cell of the $Cu_2(BO_3)_2$ plane and (c) the corresponding ^{11}B NMR spectrum at 6 T and 5 K. (d) Magnetic superlattice in the 1/3 plateau with 3 different ^{11}B sites (smallest spheres). White and black spheres represent negative and positive spin polarization, their size the magnitude. (e) ^{11}B NMR spectrum at 54 T and 2 K.

P-1

A study of ESR chromatography by means of the inverse transformation

Takayuki Suzuki

JEOL RESONANCE Inc., Akishima 196-8558, Japan.

Email: taksuzuk@jeol.co.jp

The separation of mixed spectra is very important for obtaining the correct information. DOSY and ROSY in NMR spectroscopy are well-known as methods which can separate mixed spectra **[1] [2]**. These methods generate a relaxation spectrum by the numerical inverse transformation like Inverse Laplace Transformation (ILT). In ESR field, 2D-REFINE method has been reported as a similar scheme **[3]**.

All above schemes need an input dataset measured by pulsed ESR/NMR techniques. Unfortunately, most of the paramagnetic/ferromagnetic species, which have very short relaxation times in standard state, are not suitable for such measurement techniques. In addition, least mean square fitting is usually adopted to obtain the relaxation spectra in the course of data processing. This procedure has to be predicted the number of components.

CONTIN is a well-known computer program package for the numerical inverse transformation **[4]**. There is no need to predict the number of unknown components in this program. Perturbative LOD-T_1 method, which has been reported recently **[5],** can measure the exponential decaying data based on spin-lattice relaxation in standard state. This work is an attempt to separate a mixed ESR spectrum by means of CONTIN program. Simulated two dimensional spectra shown in Fig.1 support the possibility of separation of ESR spectra, if we can obtain the appropriate decaying data. In order to confirm this prediction, we had a two dimensional perturbative LOD-T_1 experiment and converted the obtained data by means of successive CONTIN processing. As a result, a two dimensional relaxation spectrum based on LOD-T_1 scheme was obtained.

[1] K. F. Morris, C. S. Johnson, Jr., J. Am. Chem. Soc., 114 (1992) 3139-3141

[2] Y. Nishiyama, M. H. Frey, S. Mukasa, H. Utsumi, J. Magn. Res. 202 (2010) 135-139

[3] A. Cernescu, T. Maly, T. F. Prisner, J. Magn. Res. 192 (2008) 78-84

[4] S.W. Provencher, Comput. Phys. Commun. 27 (1982) 213-227

[5] T. Suzuki, J. Magn. Res. 259 (2015) 95-101

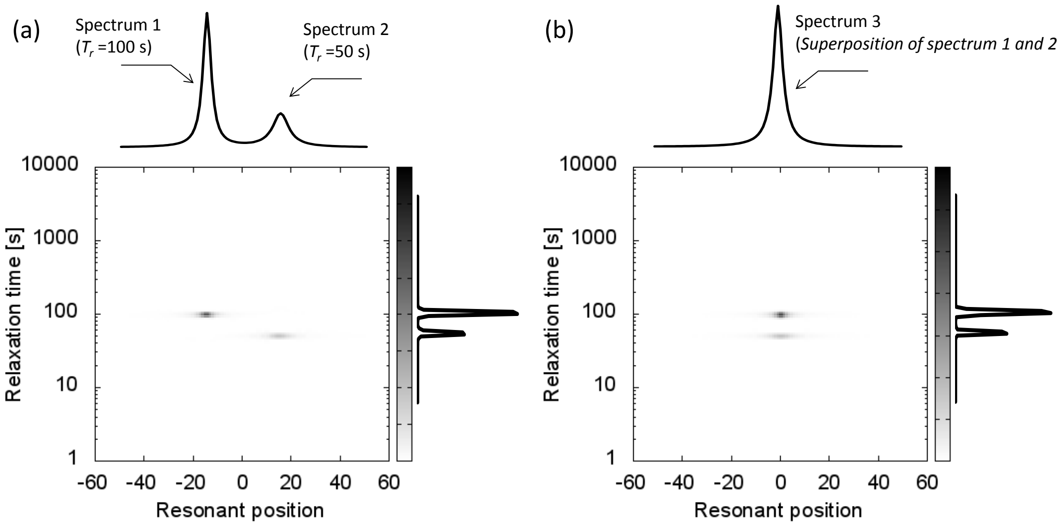

Fig. 1: Results of the CONTIN simulation of two mixed spectra.

P-2

Time-resolved EPR Study on the Photoreaction and Radical Dynamics of 9,10-Anthraquinone-2,6-Disulfonate and Ascorbic Acid at Bilayer Interface

F. Ema,[1] Z. Fu,[2] and H. Murai[3]

[1]Graduate School of Science, Kobe University, Kobe 657-8501, Japan.
[2]Graduate School of Science and Engineering, Tokyo Institute of Technology, Tokyo 152-8551, Japan.
[3]Graduate School of Science, Shizuoka University, Shizuoka 422-8529, Japan.
Email: fema@stu.kobe-u.ac.jp

Antioxidant ability of the various substances such as health foods, supplements, and anti-aging ingredients have widely attracted attention. Ascorbic acid widely known as vitamin C is one of the most important and popular antioxidant. Many antioxidant effects on our body are considered to act at biomembrane interface region. Previous study using micelle and reversed micelle sysytems as a biomembrane model indicated that the reactivity of antioxidants at the membrane interface depends on the size and the pH of the reaction field [1-3]. However, the detailed reaction mechanism and the dynamics of the radical species at the interface have not been deeply clarified [3]. Biomembrane is mainly composed of phospholipid and protein molecules. Liposome is used as an artificial biological membrane model for physiological tissue because of the similarity to the phospholipid bilayer membrane.

In this study, we studied the photoreaction of ascorbic acid (AscH$_2$) and the excited triplet state of 9,10-anthraquinone-2,6-disulfonate dianion (^{3}AQDS^{2-*}) in the cationic didodecyldimethyl ammonium bromide (DDAB) vesicle solution, using a time-resolved EPR method in combination with UV-vis absorption spectroscopy. X-band time-resolved EPR (TR-EPR) measurement was performed without magnetic field modulation at room temperature. The sample solution was deoxygenated by nitrogen gas bubbling before and during the measurement, and it flowed through a 0.3 mm flat quartz cell installed in the microwave resonator. A nanosecond-pulsed Nd:YAG laser (Continuum, Minilite; λ = 355 nm) was used as an excitation light.

TR-EPR spectrum of the DDAB vesicle system showed a totally emissive polarization due to the triplet mechanism (TM) of the chemically induced dynamic electron polarization (CIDEP). This means that ^{3}AQDS^{2-*} reacts fast with AscH$^-$ and transfer the spin polarization of ^{3}AQDS^{2-*} before spin relaxation. The contribution of the radical pair mechanism (RPM) was not apparently confirmed, indicating that the diffusion of the generated radical species is limited at the cationic bilayer interface. Analysis of UV-vis absorption and time-resolved EPR spectra revealed the formation of the intermolecular charge transfer (CT) complex of weakly bounded Asc$^{\bullet-}$and strongly trapped AQDSH$^{2\bullet-}$ at the cationic bilayer interface, and a hydrogen abstraction reaction takes place between them. These results show that the strong oxidative ability of the excited triplet states of the particular quinones is extinguished by ascorbic acid both stabilized around the cationic bilayer surface boundary.

We are grateful to Prof. Yasuhiro Kobori (Kobe University) and Dr. Tomoaki Miura (Niigata University) for many supports and useful discussions.

[1] K. Ohara, R. Watanabe, Y. Mizuta, Y. Nagaoka, and K. Mukai, J. Phys. Chem. B **107** (2003) 11527
[2] K. Ohara, Y. Hashimoto, C. Hamada, and S. Nagaoka, J. Photochem. Photobiol. A: Chem. **200** (2008) 239.
[3] X. Xu, L. Shi, Y. Liu, X-H. Ji, and Z-F. Cui, Chi. J. Chem. Phys. **24** (2011) 150.

P-3

Time resolved EPR study on the orientation of the primary charge separated state of the quinone-depleted PSII reaction center

R. Minobe[1], M. Hasegawa[1], T. Sakai[2], H. Nagashima[2], S. Katagiri[3],
T. Tachikawa[1], H. Mino[2], Y. Kobori[1]

[1]*Graduate School of Science, Kobe University, Kobe 657-8501, Japan.*
[2]*Graduate School of Science, Nagoya University, Nagoya 464-8602, Japan.*
[3]*Graduate School of Science, Shizuoka University, Shizuoka 422-8529, Japan.*
Email: 160s221s@stu.kobe-u.ac.jp

The photosynthesis has attracted a lot of attentions for a long time to understand how the plants utilize the sunlight for the highly efficient solar energy conversions. Photosystem II (PSII) reaction center plays an important role on the efficient electron transfer process to cause the chemical energy to oxidize water molecules in the process of photosynthesis. However, no experimental studies have been performed to characterize geometries and electronic couplings of the primary CS states, although kinetics of the primary charge separation (CS) and the recombination processes have been observed by using the optical spectroscopy in the PSII reaction center. We have herein employed a time resolved EPR (TREPR) method to clarify the geometries of the primary charge-separated state and of the excited triplet state generated by the primary charge-recombination (CR) in the PSII reaction center in which the secondary electron acceptors of quinones are depleted.

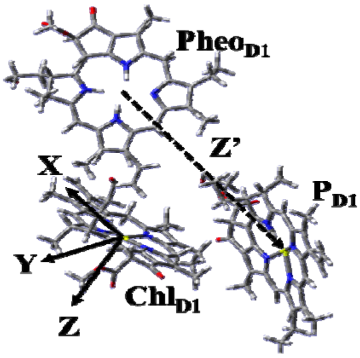

Fig. 1: X-ray structure of the co-factors in the PSII reaction center

Fig. 2 shows the TREPR spectra obtained by a nanosecond 532 nm laser irradiations of the quinone-depleted PSII reaction center from spinach at 77 K. The primary CS state composed of P_{D1} radical cation in the special pair and pheophytin ($Pheo_{D1}$) radical anion is known to be generated after the light excitation (Fig. 1). In the quinone-depleted system, the forward electron-transfer reaction is blocked at $Pheo_{D1}$ and therefore, the primary CS state is deactivated by the triplet recombination. At the delay time of 0.8 μs, we observed the broad spectrum with a spin polarization pattern of A/E/E/A/A/E. This spectrum polarization pattern is a signature of the excited triplet state of Chl_{D1} generated by the triplet charge recombination via the S-T_0 mixing. As delay time goes on, another peaks gradually appeared around 325 mT and 355 mT. Based on the position of the peaks, these signal are assigned to the triplet state of $Pheo_{D1}$ indicating that the energy transfer from ^{3}Chl* to ^{3}Pheo* occurred after the primary CR. We have modeled the time-evolutions of the transverse magnetizations of the ^{3}Chl* using the stochastic-Liouville equation [1] and determined the orientational structures of the initial CS state and of the triplet state.

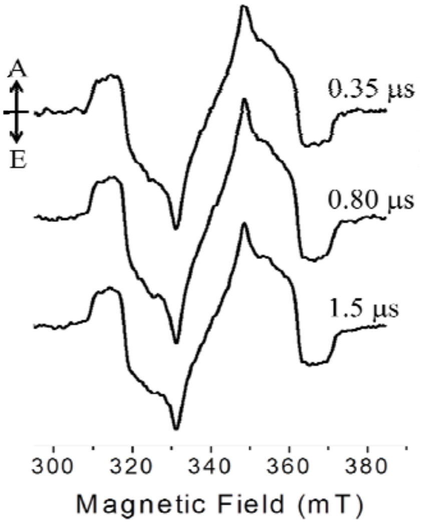

Fig. 2: TREPR spectra of the quinone -depleted PSII reaction center obtained at 77 K.

[1] Kobori, Y.; Ponomarenko, N.; Norris, J. R. Jr. *J. Phys. Chem. C*, **2015**, *119*, 8078–8088.

Terahertz ESR measurement of Metalloporphyrin Complexes

T. Okamoto,[1] H. Takahashi,[2] E. Ohmichi,[1] and H. Ohta[3]

[1]*Graduate School of Science, Kobe University, Kobe 657-8501, Japan.*

[2]*Organization for Advanced and Integrated Research, Kobe University, Kobe 657-8501, Japan.*

[3]*Molecular Photoscience Research Center, Kobe University, Kobe 657-8501, Japan.*

Email: t-okamoto@stu.kobe-u.ac.jp

ESR measurement in the terahertz (THz) region has great advantages such as high g-value resolution and observation of the large zero-field gap. Also, THz ESR at multiple frequencies is useful to study the electronic structure of a sample in the view of spectroscopy. However, because the output power of THz light sources is usually low, and hence mg-order sample mass is needed. For this reason, it is very difficult to attain sufficient sensitivity for metalloproteins, since preparation of a large amount of sample volume needs substantial efforts.

To reduce sample volume and obtain high sensitivity in THz ESR measurement, we have developed a novel ESR technique using a microcantilever [1-4]. A unique feature of this technique is that a sample mass only on the order of 100 ng – 10 μg is needed. In this technique, a tiny amount of a sample is mounted on a microcantilever end and electromagnetic waves are irradiated onto the microcantilever in the presence of a static external magnetic field. A ferromagnetic rod, which produces a magnetic field gradient at the sample position, is located above the sample. The optical fiber end is located beneath the microcantilever separated by ~100 μm. Therefore, Fabry-Perot cavity is formed between the fiber end and the microcantilever surface. When ESR transition occurs, the corresponding magnetization change is detected by Fabry-Perot interferometry as a cantilever bending.

Figure 1 shows a schematic of the experimental setup of our microcantilever ESR system. A dysprosium rod was used to make a field gradient on the order of 1000 T/m. To extend the dynamic range, we used a feedback system to keep the interference intensity of the Fabry-Perot cavity constant using a tunable laser [5]. In this study, we applied our technique to metalloporphyrin complexes: Cu-TPP (Cu^{2+}, $S = 1/2$) and hemin (Fe^{3+}, $S = 5/2$), where TPP is tetraphenylporphyrin. The sample mass was about 100 ng in both cases. All ESR measurements were performed at 4.2 K. We successfully observed ESR signals of Cu-TPP and hemin in the frequency range of up to 0.4 and 0.5 THz, respectively. From these results, we determined the zero-field splitting parameter of hemin. In the presentation, we will show the details of our apparatus and multi-frequency ESR results of these metalloporphyrin complexes.

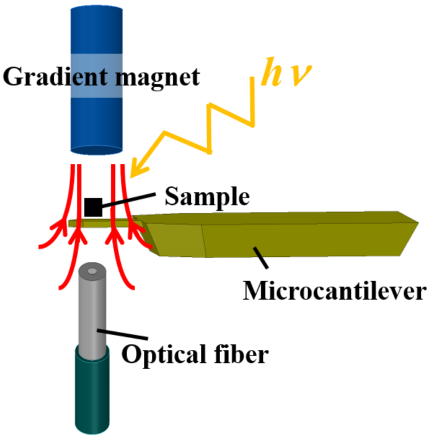

Fig. 1: Schematic of our experimental setup.

[1] E. Ohmichi, N. Mizuno, M. Kimata, and H. Ohta, Rev. Sci. Instrum. **79** (2008) 103903/1-7.
[2] E. Ohmichi, N. Mizuno, M. Kimata, H. Ohta, and T. Osada, Rev. Sci. Instrum. **80** (2009) 013904/1-6.
[3] E. Ohmichi, Y. Tokuda, R. Tabuse, D. Tsubokura, T. Okamoto, and H. Ohta, Rev. Sci. Instrum. **87** (2016) 073904/1-8.
[4] T. Okamoto, H. Takahashi, E. Ohmichi, and H. Ohta, to appear in J. Infrared Milli. and Terahz. Waves. (2016).
[5] H. Takahashi, T. Okamoto, E. Ohmichi, and H. Ohta, to appear in Appl. Phys. Express.

P-5

Fabrication of Fabry-Perot type cantilever for high-sensitivity force-detected ESR measurement

Toshihiro Miki,[1] Eiji Ohmichi ,[1] Hitoshi Ohta [2]
[1]*Graduate School of Science, Kobe University, Kobe 657-8501, Japan.*

[2]*Molecular Photoscience Research Center, Kobe University, Kobe 657-8501, Japan.*

Email: 151s125s@.kobe-u.ac.jp

In our group, a sensitive ESR measurement technique using a micro-cantilever has been developed. In this technique, ESR signal is force-detected as a cantilever bending caused by the magnetization change associated with ESR absorption. This force-detected ESR technique allows sensitive measurements of a tiny amount of sample volume in the millimeter-wave and terahertz region. In this study, we fabricated ultra-thin cantilevers using a microfabrication process and apply them to force-detected ESR measurements in the millimeter-wave region.

We used SOI (silicon-on-insulator) wafers to fabricate micro-cantilevers with standard fabrication processes such as photolithography, evaporation, dry etching, wet etching. Figure 1 shows a Fabry-Perot type cantilever, in which the cantilever displacement is detected by an optical fiber placed beneath the cantilever. Cantilever thickness was 2μm or 0.3μm, and the length was about 450μm. Characterization of the fabricated cantilevers were carried out by the thermal oscillation spectrum. From the analysis, the eigenfrequency was about 13.5 KHz, and the lowest spring constant was estimated to be 0.002 N/m. This value is smaller than those of commercial cantilevers, and better detection sensitivity is expected.

We applied these cantilevers to high-frequency ESR measurement, and successfully obtained force-detected ESR signals at 80, 90, and 105 GHz for DPPH, as shown in Fig. 2. Spin sensitivity, estimated from the signal to ratio, was about 10^{12} spins/Gauss.

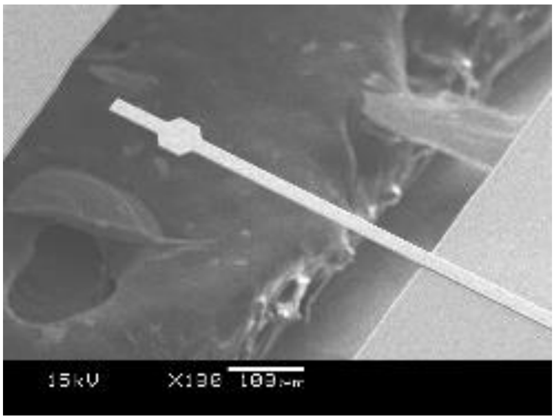

Fig. 1: SEM image of 2-μm thickness cantilever

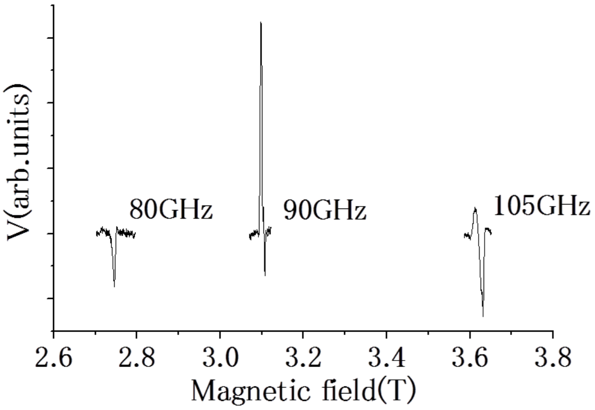

Fig. 2: Force-detected ESR spectra of DPPH at 4.2K

P-6

Development of a piezoelectric translational stage for magnetic resonance force microscopy

A. Miyazaki[1], E. Ohmichi[1], and H. Ohta[2]

[1]*Graduate School of Science, Kobe University, Kobe 657-8501, Japan.*

[2]*Molecular Photoscience Research Center, Kobe University, Kobe 657-8501, Japan.*

Email: swingin.pengin@gmail.com

Terahertz cantilever-detected ESR is a sensitive method of high-frequency ESR technique using a micro cantilever. In this technique, ESR signals are detected by a magnetization change of the sample associated with ESR transition.

Magnetic resonance force microscopy (MRFM) is a kind of scanning probe microscopy combined with magnetic resonance (MR) imaging technology [1-3]. A high spatial resolution is obtained by scanning a magnetic tip on a cantilever over the sample surface. Our aim is to develop MRFM technique in the terahertz region to realize better spectral resolution. For this purpose, we developed a three-axis piezoelectric translational stage for MRFM, based upon a stick-and-slip mechanism. In this system, saw-tooth waves are applied to the piezoelectric element, and the stage is driven by the difference between static and dynamic friction forces acting between the stage and a sapphire rod (Fig. 1).

Characterization of the stage was carried out at room temperature, 77K, and 4K, and the results are shown in Fig.2 . The travel distance per pulse was ~700 nm at 90 V, but it decreased with decreasing temperature. In this presentation, we will report the design, construction and the performance of the devices in details..

[1]S. Tsuji *et al*, Journal of Magnetic Resonance 188 (2007) 380–386.
[2]Z. Zhang *et al*, Solid State Nuclear Magnetic Resonance 11 (1998) 65–72.
[3]C. L. Degen *et al*, PNAS 106(2009) 1313-1317.

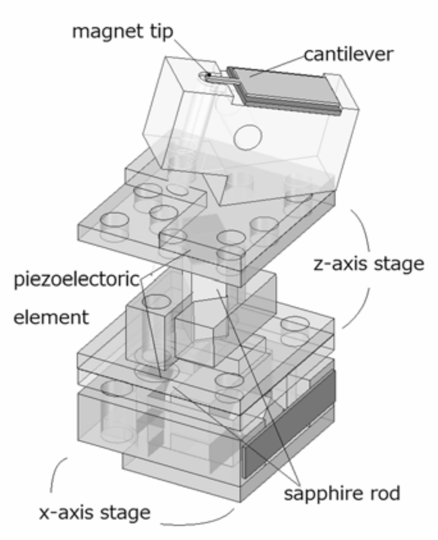

Fig. 1: Schematic of the piezoelectric stages mounting a cantilever holder.

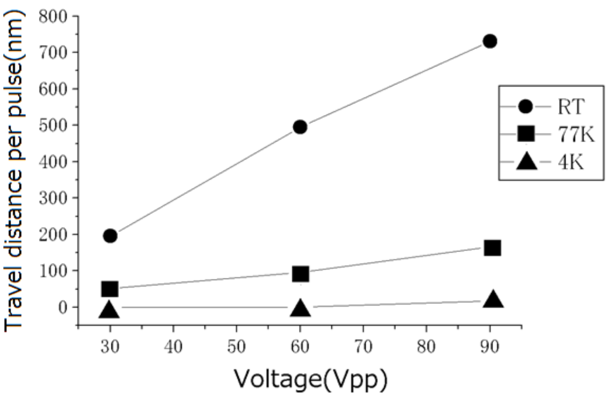

Fig. 2 Travel distance per pulse of the piezoelectric z-axis

Development of a microforce measurement apparatus using a cantilever

H. Horie,[1] E. Ohmichi,[1] and H. Ohta[2]

[1]*Graduate School of Science, Kobe University, Kobe 657-8501, Japan.*

[2]*Molecular Photoscience Research Center, Kobe University, Kobe 657-8501, Japan.*

Email: 163s118s@stu.kobe-u.ac.jp

Microforce measurement is one of the most important techniques in modern physics. For this purpose, micro-cantilever is useful in that microforce can be detected as a cantilever deflection. The deflection of a cantilever is sensitively measured by a fiber-optic Fabry-Perot interferometer.

One of such applications is force-detected electron spin resonance (ESR). It is noted that electron population of up and down spins changes at ESR absorption, resulting in a magnetization change of a sample. This change can be detected as a field gradient force acting on the sample in the presence of a gradient field.

Another application is Casimir force measurement. Casimir force is an attractive force originating from the zero-point fluctuation in vacuum. In this case, a force acting between a metal plate and a metal-coated sphere fixed on a cantilever has to be sensitively measured with an accuracy of 1 pN.

For these purposes, we developed a microfoce measurement system using a cantilever. The optical system is shown in Fig. 1. A super-luminescent diode (SLD) (nominally 1310 nm wavelength) with high wavelength stability and low coherence length was used as a light source. Due to its short coherence length, spurious interference was substantially decreased. The interferometer cavity was formed between an end of the fiber and a back surface of the cantilever. Three small translational stages were assembled in order to adjust the fiber position relative to the cantilever. Cantilever displacement was measured as a change of the interference intensity. With this system, a cantilever displacement on the order of 1 pm could be detected.

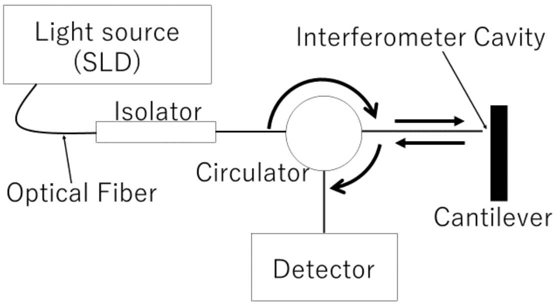

Fig. 1: Schematic diagram of the fiber-optic interferometer developed in this study.

P-8

ESR study of kagome like frustrated magnet $K_2Mn_3(OH)_2(VO_4)_2$

M. Fujimoto,[1] S. Okubo,[1, 2] S. Hara,[3] T. Sakurai,[3] H. Ohta,[1, 2] D. Otuka,[4] and H. Sato[4]

[1]*Graduate School of Science, Kobe University, Kobe 657-8501, Japan*
[2] *Molecular Photoscience Research Center, Kobe University, Kobe 657-8501, Japan*
[3]*Center for Supports to Research and Education Activities, Kobe University, Kobe 657-8501, Japan*
[4]*School of Science and Engineering, Chuo University, Tokyo 112-8551, Japan*

Email: 167s116s@stu.kobe-u.ac.jp

$K_2Mn_3(OH)_2(VO_4)_2$ is two dimensional antiferromagnetic substance. Magnetic ion of $K_2Mn_3(OH)_2(VO_4)_2$ is Mn^{2+} ($S = 5/2$), which has diamond chain and kagome like structure as called as MKS (Multi-Kagome-Strip) lattice. Magnetic frustration is expected due to including triangular structure in MKS lattice (Fig. 1) [1]. MKS lattice has three different exchange interactions due to three different nonequivalent sites. Therefore, different magnetic phases of ground state are expected to depend on three interactions. If we consider that all exchange interactions are antiferromagnetically, the magnetic structure of the ground state can be divided into three phases, chiral state, ferri magnetic state, and one-dimensional antiferromagnetic state. $K_2Mn_3(OH)_2(VO_4)_2$, which was synthesized by Otuka *et al.*, is one of the model substance for MKS lattice antiferromagnet. Temperature dependence of magnetic susceptibility under the magnetic field of 3 T indicated a broad maximum at 80 K and antiferromagnetic phase transition at 50 K [2]. The weiss temperature was estimated to be -375 K [2].

We performed ESR measurements of $K_2Mn_3(OH)_2(VO_4)_2$ single crystal to obtain information of magnetic anisotropy. To clarify the magnetic anisotropy of paramagnetic state, the angular dependence of linewidth and g-value have been experimented using X-band ESR equipment at room temperature. Furthermore, the temperature dependence measurements for $H \perp bc$ plane have been performed in the temperature range from 4.2 K to 300 K. In addition, to measure the magnetic anisotropy of antiferromagnetic state, the frequency dependence of ESR measurements in submillimeter wave region have been performed at 4.2 K in the frequency range from 40 GHz to 550 GHz. In Fig. 2 we exhibit the angular dependence of linewidth from perpendicular to the plane a^* to in-plane direction(*c-axis*) for X-band ESR measurements. The angular dependence of linewidth shows a extra minimum between $H//a^*$ and $H//c$. Consider the magnetic dipole interactions in two dimensional square lattice, the angular dependence of linewidth is expressed $\Delta H \propto (3\cos^3\theta - 1)^2 + (const.)$ [3]. In particular, in the case of $\theta = 55°$, linewidth takes minimum value due to $3\cos^3\theta - 1 = 0$, which means that the magnetic dipole interaction minimalize at $\theta = 55°$. Lineshape shows coincidentally lorentzian shape at $\theta = 55°$. As shown in the Fig. 2, it shows that $K_2Mn_3(OH)_2(VO_4)_2$ is good two dimensional magnetic substance. We will report also details of magnetic anisotropy in connection with previous research.

[1] J-H. Liao, *et al.* Acta Crystallogr. **C52** (1996) 284
[2] D. Otsuka *et al.*, Meeting abstracts of the Physical Society of Japan (Sept. 2014) Part3, p312
[3] P M Richards, *et al.* Phys. Rev. **B9** (1974) 32

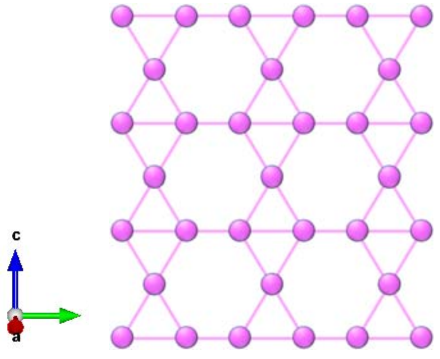

Fig. 1: Schematic view of the MKS lattice.

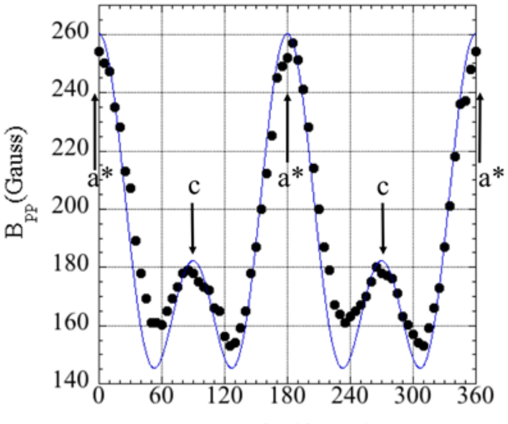

Fig. 2: The angular dependence of linewidth at room temperature.

Spin dynamics of two-dimensional square lattice magnet $Sr_2MnO_2Cl_2$

A. Takahashi[1], S. Okubo[1, 2], S. Hara[3], T. Sakurai[3], H. Ohta[1, 2], E. Matsuoka[1], H. Sugawara[1], Y. Tsujimoto[4], S. Yu[4], K. Yamaura[4]

[1]*Graduate School of Science, Kobe University, Kobe 657-8501, Japan*

[2]*Molecular Photoscience Research Center, Kobe University, Kobe 657-8501, Japan*

[3]*Center for Supports to Research and Education Activities, Kobe University, Kobe 657-8501, Japan*

[4]*National Institute for Materials Science, Tsukuba 305-0047, Japan*

Email: takahashiaki0423@gmail.com

Since Haldane has conjectured existence of an energy gap between the ground state to first excited state in *S*=1 one-dimensional antiferromagnet, low-dimensional spin systems have been attracted much attention to strong quantum fluctuation effect. The crystal structure of $Sr_2MnO_2Cl_2$ is a tetragonal as shown in fig. 1. Mn^{2+} ($3d^5$) ions of $Sr_2MnO_2Cl_2$, which are located at center of a square of oxygen, forms square lattice. The exchange interaction between Mn ions is expected to have an antiferromagnetic interaction due to 180º angle of Mn-O-Mn from the Goodenough-Kanamori rule. However, there is no sign of antiferromagnetic order down to 2 K in the magnetic susceptibility measurement. From the Currie-Weiss fitting between 200 K~400 K, the Weiss temperature is estimated to be +1.5 K [1]. We have already reported development of short range order below 20 K from observation of the g-shifts in ESR measurements of powder and magnetically oriented (*H* // *c*-axis) samples [2]. In this paper, we report ESR measurements of a new oriented samples (*H* // *ab*-plane). Fig. 2 shows the temperature dependence of the ESR spectra for *H* // *ab*-plane observed in 240 GHz. Resonance field begins to shift below 70K, and the linewidth increases as the temperature decreases. Furthermore, the obtained g-values were different from that of the powder and the magnetically oriented (*H* // *c*-axis) samples.

[1] Y. Tsujimoto, *et al.*, Chem. Commun. **50** (2014) 5915-5916

[2] A. Takahashi, *et al.*, abstract of meeting of Physical Society of Japan (2016). 20pBC-9 ISSN: 2189-079X

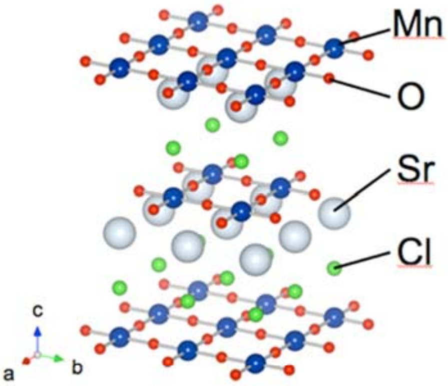

Fig. 1 Crystal structure of $Sr_2MnO_2Cl_2$

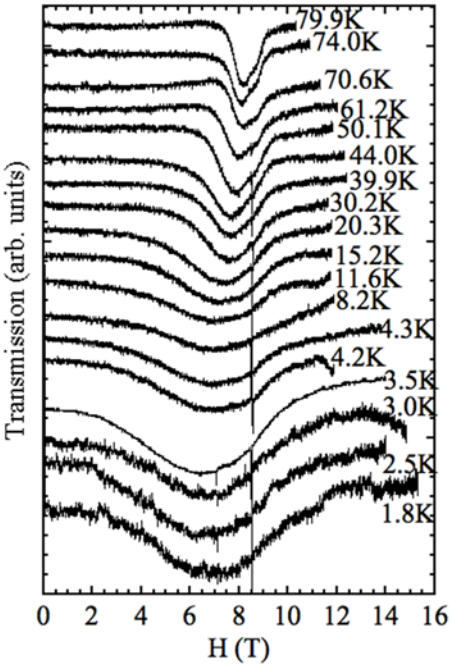

Fig. 2 The temperature dependence of the ESR spectra of the magnetically oriented sample (*H* // *ab*-plane) for 240GHz

P-10

Submillimeter wave ESR measurements of *S*=1/2 distorted diamond chain $Cu_3(OH)_2(CH_3CO_2)_2(H_2O)_xX_y$

Daisuke Miyazaki,[1] Khalif Benzid,[2] Susumu Okubo,[1, 2] Shigeo Hara,[3] Takahiro Sakurai,[3]
Hitoshi Ohta,[1, 2] Wataru Fujita[4]

[1]*Graduate School of Science, Kobe University, Kobe 657-8501, Japan*

[2]*Molecular Photoscience Research Center, Kobe University, Kobe 657-8501, Japan*

[3]*Center for Supports to Research and Education Activities, Kobe University, Kobe 657-8501, Japan*

[4]*Department of Information and Basic Science, Graduate School of Natural Science, Nagoya City University, Nagoya 467-8501, Japan*

Email: daisuke.1641@gmail.com

One-dimensional quantum spin systems have much attention to existence of large quantum fluctuation in the ground state. In especially, *S*=1/2 antiferromagnetic diamond chain has low-dimensionality and geometrical spin frustration effect due to existence of triangular structure. Three different ground states depending on the strength of the interactions have been proposed by Okamoto[1]. $Cu_3(OH)_2(CH_3CO_2)_2(H_2O)_xX_y$ is a model compound for the *S*=1/2 distorted diamond chain. In this sample, can be taken as organic anions like 2,6-Np$(SO_3)_2$, 1,5-Np$(SO_3)_2$, and $EtC_6H_4SO_3$ (Np is naphthalene). In these compounds, different ground states of the *S*=1/2 distorted diamond chain can be compared by changing anions. Fig. 1 shows the crystal structure of 2,6-Np$(SO_3)_2$. The crystal structure of 2,6-Np$(SO_3)_2$ is orthorhombic, and its magnetic susceptibility shows a broad peak at around 70 K, and shoulder at around 20 K[2]. We have performed X-band ESR and high frequency ESR measurements to examine the magnetic anisotropy of this compound.

The result of X-band ESR, we found very broad absorption lines at around 20~50 K, and its resonance fields are about 0.4 T. But the linewidths are too broad to observe absorption line in X-band ESR. Therefore have performed high frequency ESR measurements using pulsed high magnetic field. Fig. 2 shows the temperature dependence of 2,6-Np$(SO_3)_2$ (random orientation) ESR spectra for 160 GHz. Solid circles and open squares indicate intrinsic resonance fields of the sample. Spin dynamics and the magnetic anisotropy will be discussed.

[1] K. Okamoto *et al.*, J. Phys: Cond. Matt **15** (2003) 5979-5995
[2] W. Fujita *et al.*, in preparing to publish

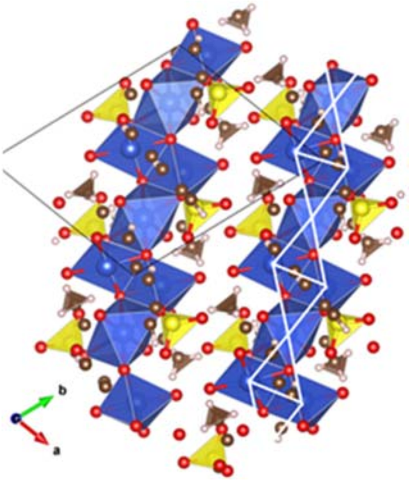

Fig. 1: The crystal structure of 2,6-Np$(SO_3)_2$

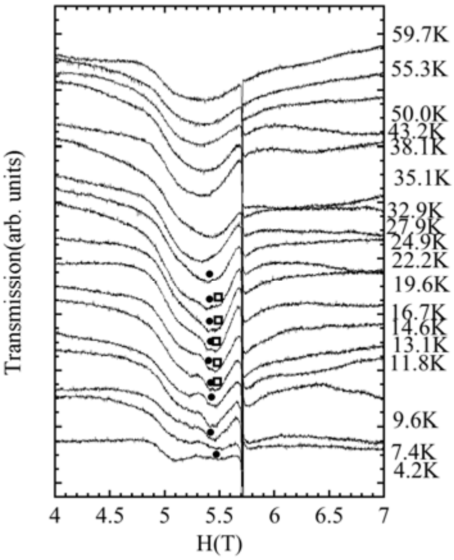

Fig. 2: temperature dependence of 2,6-Np$(SO_3)_2$ (random orientation) ESR spectra for 160GHz

P-11

Terahertz ESR measurements of Multiferroic compound $BiFe_{0.9}Co_{0.1}O_3$

A. Morimitsu[1], S. Okubo[2], S. Hara[3], T. Sakurai[3], H. Ohta[1,2], H. Yamamoto[4] and M. Azuma[5]

[1]*Graduate School of Science, Kobe University, Kobe 657-8501, Japan*

[2]*Molecular Photoscience Research Center, Kobe University, Kobe 657-8501, Japan*

[3]*Center for Supports to Research and Education Activities, Kobe University, Kobe 657-8501, Japan*

[4]*Interdisciplinary Graduate School of Science and Engineering, Tokyo Institute of Technology,*

Yokohama 226-8503, Japan

[5] *Laboratory for Materials and Structures, Tokyo Institute of Technology, Yokohama 226-8503, Japan*

Email: 156s128s@stu.kobe-u.ac.jp

Multiferroics have been formally defined as materials that exhibit more than one primary ferroic order parameter simultaneously and many researchers consider materials to be multiferroics only if they exhibit coupling between primary order parameters.

Perovskite compound $BiFeO_3$ shows antiferromagnetism and ferroelectricity below T_N=650 K and T_C=1100 K, respectively. Co doped $BiFeO_3$ has magnetic ion Fe^{3+} and non magnetic ion Co^{3+}, because Co ions lay in the low spin state [1]. Crystal structure of $BiFe_{0.9}Co_{0.1}O_3$ is rhombohedral, which is the same as the structure of $BiFeO_3$. The magnetic structure of $BiFe_{0.9}Co_{0.1}O_3$ under zero magnetic field changes from cycloidal structure to collinear structure above 220 K that have been reported by Yamamoto [1]. Fig. 1 is magnetic phase diagram of $BiFe_{1-x}Co_xO_3$. Shaded regions correspond to the cycloidal phase. The magnetic structure of $BiFe_{1-x}Co_xO_3$ changes the collinear to the cycloidal structures by magnetic field, temperature and percentage of Co concentration [2].

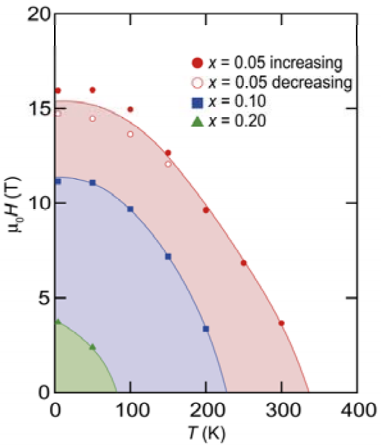

Fig. 1: Magnetic phase diagram of $BiFe_{1-x}Co_xO_3$ (x=0.05, 0.10, 0.20)[1].

Terahertz ESR measurements of $BiFe_{0.9}Co_{0.1}O_3$ have been performed to clarify the electric state of Fe^{3+} from viewpoint of microscopic measurements.

We measured $BiFe_{0.9}Co_{0.1}O_3$ powder sample were composed by high-pressure synthesis. Terahertz ESR measurements of $BiFe_{0.9}Co_{0.1}O_3$ powder have been performed by using pulsed magnetic field up to 16 T in the temperature range from 4.2 K to 265 K. The details of experiments were shown in refs.[3].

Fig. 2 is frequency dependence of ESR spectra at 4.2 K. The sharp absorptions are DPPH (g=2.0) signals for field marker. Above 408GHz, new absorptions are appears. High field absorptions have different g-values from one of low frequency absorptions. According to the frequency-field diagram at 4.2K, $BiFe_{0.9}Co_{0.1}O_3$ has phase boundary at 11 T, which is shown in broken line.

We will discuss the magnetic states of $BiFe_{0.9}Co_{0.1}O_3$ from the frequency-field diagrams measured at various temperatures.

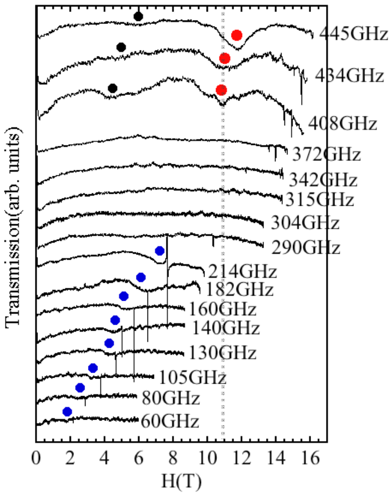

Fig. 2: Frequency dependence of ESR spectra for $BiFe_{0.9}Co_{0.1}O_3$ at 4.2 K.

[1] H. Yamamoto, *et al.*, J. Phys. Soc. Jpn. **85** (2016) 064704
[2] I. Sosnowska, *et al.*, Inorg. Chem. **52** (2013) 13269
[3] H. Ohta, *et al.* J. Phys. Conf. Serie. **51** (2006) 611

P-12

High Frequency ESR Measurements of *S*=1/2 antiferromagnetic chain $KCuMoO_4(OH)$

So Kubota[1], Shigeo Hara[2], Takahiro Sakurai,[2] Susumu Okubo,[1,3]
Hitoshi Ohta,[1,3] Kazuhiro Nawa,[4] Takashi Yajima,[5] Yoshihiko Okamoto,[6] and Zenji Hiroi[5]

[1]*Graduate School of Science, Kobe University, Kobe 657-8501, Japan*

[2]*Center for Supports to Research and Education Activities, Kobe University, Kobe 657-8501, Japan*

[3]*Molecular Photoscience Research Center, Kobe University, Kobe 657-8501, Japan*

[4] *Institute of Multidisciplinary Research for Advanced Materials, Tohoku University, Sendai 980-8577, Japan*

[5] *ISSP, University of Tokyo, Kashiwa 277-8581, Japan*

[6] *Department of Applied Physics, Nagoya University, Nagoya 464-8603, Japan*

Email: 166s108s@stu.kobe-u.ac.jp

Quantum spin systems have attracted much attention since Haldane conjecture. In particularly, many theoretical calculations have been performed in $S = 1/2$ one-dimensional Heisenberg spin systems. $KCuMoO_4(OH)$ is a new model substance for $S = 1/2$ one-dimensional Heisenberg antifferromagnet. Magnetic ion of this substance is Cu^{2+} ion $S = 1/2$, which forms one-dimensional chains. Figure 1 is the crystal structure of $KCuMoO_4(OH)$ (hydrogen atoms are omitted). $CuO_4(OH)_2$ octahedra share their edges to form *a* spin chain along the *b*-axis. The crystal structure is an orthorhombic structure with the space group *Pnma* [1]. The Weiss temperature is estimated to be -205 K from the magnetic susceptibility for H//*a*[1].

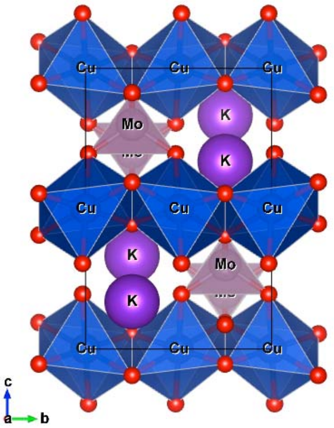

Figure 1 Crystal structure of $KCuMoO_4(OH)$

Antiferromagnetic superexchange interaction and Dzyaloshinsky-Moriya interaction with staggered D vector between spins are expected in $KCuMoO_4(OH)$. There are a few experimental reports of breather excitation, which is bound state of soliton-antisoliton pair. Therefore, we try to observe a breather excitation in $S = 1/2$ antiferromagnetic chain $KCuMoO_4(OH)$.

High-frequency ESR measurements of $KCuMoO_4(OH)$ poly crystals have been performed using pulsed magnetic field up to 16 T. Measured frequency range is from 50 GHz to 240 GHz. The temperature range was from 75 K to 1.8 K. Figure 2 shows the temperature dependence of ESR spectra from 75 K to 1.8 K. A broad absorption line at around $g = 2$ is extrinsic signal. Below 12 K new absorption appears at around 1 T. The frequency dependence of the absorption lines will be discussed in connection with the breather excitation of Cu-benzoate.

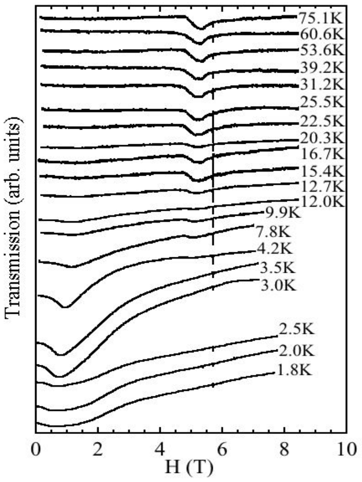

Figure 2 Temperature dependence of ESR spectra for 160 GHz

[1] K. Nawa, T. Yajima, Y. Okamoto, and Z. Hiroi, Inorg. Chem. **54**, 5566 (2015)

P-13

High pressure THz ESR measurements of spin-gap system $KCuCl_3$

Y. Hirao,[1] E. Ohki,[1] T. Sakurai,[2] H. Ohta,[3] S. Okubo,[3]
Y. Uwatoko,[4] and H. Tanaka[5]

[1]*Graduate School of Science, Kobe University, Kobe 657-8501, Japan.*
[2]*Molecular Photoscience Research Center, Kobe University, Kobe 657-8501, Japan.*
[3]*Center for Supports to Research and Education Activities, Kobe University, Kobe 657-8501, Japan.*
[4]*The Institute for Solid State Physics, University of Tokyo, Kashiwa 277-8581, Japan.*
[5]*Graduate School of Science, Tokyo Institute of Technology, Meguroku 152-8550, Japan*
Email: 157s122s@stu.kobe-u.ac.jp

High pressure ESR measurement in THz region [1] is a powerful means to study so-called spin gap system. The spin gap system has the energy gap between the non-magnetic ground state and excited state, and the ESR mode due to the direct transition between these states is sometimes observed. The high pressure ESR can clarify the precise pressure dependence of the gap energy.

$KCuCl_3$ is one of the typical spin gap systems which consist of S = 1/2 antiferromagnetic dimers. ground state is the singlet and the excited state is triplet. In the high-field ESR measurements, the ESR transition modes were observed very clearly and the gap energy was estimated to be 640 GHz [2]. The pressure effect on such spin gap system was studied theoretically [3]. It is expected that the novel ESR mode called as amplitude mode appears above the critical pressure P_c when the gap is collapsed applying pressure. From the magnetization measurement under pressure P_c was estimated to be 0.82 GPa [4]. In order to obtain the detailed information for the pressure effect and to observe the mode, we have performed the high pressure THz ESR measurement of this compound up to 1 GPa.

Figure shows the frequency dependence ESR spectra obtained at 0.6 GPa. Below 380 GHz, we observed rather broad signal indicated by triangle. was assigned to the signal due to the direct transition from the $S = 0$ state to the $S_z = 1$ of $S = 1$ states. The gap energy is estimated to be around 220 GHz at 0.6 GPa and it clearly shows the reduction of the gap energy by the pressure. The corresponding critical field is about 7.2 T. The absorption lines indicated by circle in Fig. shows clear change of ESR mode above this field. It also supports the reduction of the gap energy. The detailed including results obtained at around critical pressure will be presented.

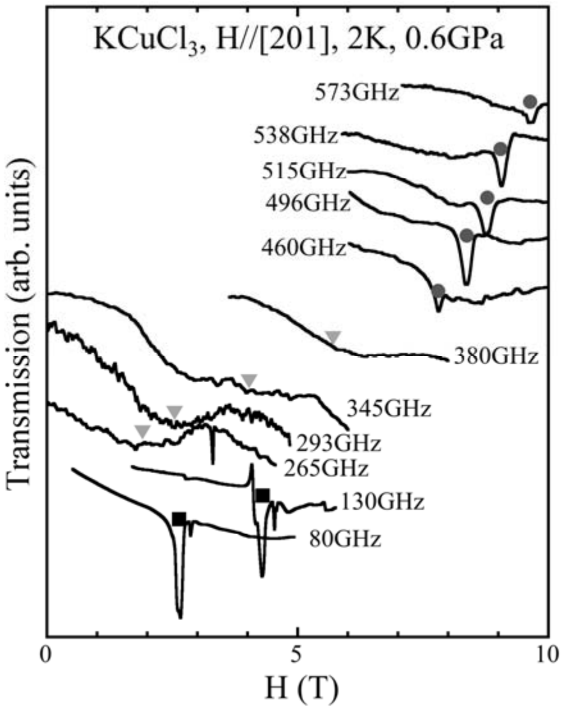

Fig. Frequency dependence ESR spectra obtained at 0.6 GPa and 2 K for H||[201].

[1] T. Sakurai *et al.*, J. Magn. Reson. **259** (2015) 108.
[2] S. Kimura *et al.*, Physica. B **346-347** (2004) 15-18.
[3] M. Matsumoto *et al.*, Phys. Rev. B **69** (2004) 054423.
[4] K. Goto *et al.*, J. Phys. Soc. Jpn. **76** (2007) 162.

P-14

Development of high pressure and high field ESR system and its application to quantum spin system

E. Oki[1], T. Sakurai[2], Y. Hirao[1],
S. Okubo[3], H. Ohta[3], Y. Uwatoko[4], H. Tanaka[5], A. Sera[6,7], Y. Takasaka[6,7],
J. Akimitsu[6,7], M. Sera[9] and K. Inoue[6,7,8]

[1]*Graduate School of Science, Kobe University, Kobe 657-8501, Japan.*
[2]*Center for Supports to Research and Education Activities, Kobe University, Kobe 657-8501, Japan.*
[3]*Molecular Photoscience Research Center, Kobe University, Kobe 657-8501, Japan.*
[4]*Institute for Solid State Physics, Tokyo University, Chiba 277-8581, Japan.*
[5] *Graduate School of Science, Tokyo Institute of Technology University, Tokyo 152-8551, Japan.*
[6]*Graduate School of Science, Hiroshima University, Hiroshima 739-8511, Japan.*
[7]*Center for Chiral Science, Hiroshima University, Hiroshima 739-8526, Japan.*
[8]*Institute for Advanced Materials Research, Hiroshima University, Hiroshima 739-8511, Japan.*
[9]*Graduate School of Advanced Science of Matter, Hiroshima University, Hiroshima 739-8511, Japan.*
Email;ohki0502@gmail.com

Triangular lattice antiferromagnet $CsCuCl_3$ is a well-known material which shows a quantum phase transition from the 120° spin structure to the coplanar structure below $T_N = 10.7$ K in a magnetic field parallel to the *c*-axis [1]. Recently, it has attracted much attention again since a 1/3 plateau was found in its magnetization curve under pressure of about 0.7 GPa [2]. The purpose of this study is to clarify the details of this pressure effect on $CsCuCl_3$.

The high pressure ESR is a powerful tool to investigate the spin states under pressure from the microscopic point of view. Although we have a high pressure ESR system whose maximum magnet field 10 T [3], a new high pressure ESR is required as the 1/3 plateau is observed around 15 T. Therefore, we have developed a new reflection-type high pressure ESR system. In this system, the incident light which passes through a sample in the pressure cell is reflected by a mirror set at the bottom of the sample space and this reflected light is detected by the detector placed outside the cryostat. This system is applicable to various type magnets and we will try to apply it to the pulse magnet.

We also performed high pressure ESR measurements of this material up to 10 T by the old system. The antiferromagnetic resonance (AFMR) mode which is peculiar to the 120° structure was observed up to 2.5 GPa clearly. Figure 1 shows the pressure dependence of the antiferromagnet gap at zero field and it shows the large increase by applying pressure. In order to clarify the origin of this increase, we try to separate the parameters which compose the antiferromagnet gap by using other pressure dependence measurements.

We will show the detailed results in addition to the outline of the new high pressure ESR system.

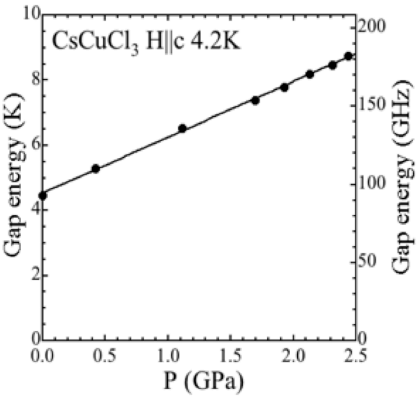

Fig. 1 Pressure dependence of antiferromagnet gap of $CsCuCl_3$.

[1] T. Nikuni and H. Shiba, J. Phys. Soc. Jpn. 62 (1993) 3268.
[2] A. Sera, private communication.
[3] T. Sakurai *et al*., J. Magn. Reson. 259 (2015) 108.

P-15

ESR study of nonmagnetic impurity effect of S=1/2 two legs spin ladder antiferromagnet $[Ph(NH_3)](18\text{-crown-}6)[Ni(dmit)_2]_{1-x}[Au(dmit)_2]_x$

Khalif Benzid[1], Atsushi Asakura[2], Masashi Fujisawa[3], Susumu Okubo[1,2], Hitoshi Ohta[1,2], Sadafumi Nishihara[4,5], Tomoyuki Akutagawa[6], Takayoshi Nakamura[6], Yuko Hosokoshi[7], and Katsuya Inoue[4,5]
[1]Molecular Photoscience Research Center, Kobe University, Kobe, 567-8501, Japan
[2]Graduate School of Science, Kobe University, Kobe, 567-8501, Japan
[3]Department of Frontier Research and Technology, Kobe University, Kobe, 567-8501, Japan
[4]Graduate School of Science, Hiroshima University, Hiroshima, 739-8526, Japan
[5]Institute for Advanced Materials Research, Hiroshima University, Hiroshima, 739-8526, Japan
[6]Department of Physical Science, Osaka Prefecture University, Osaka, 599-8531, Japan
[7]Research Institute for Electronic Science, Hokkaido University, Sapporo, 060-0812, Japan
Email: benzid@people.kobe-u.ac.jp

Abstract

In the last decades, many studies have opened the curtain on the magnetic properties and the impurity effect on many quantum spin systems such as the Haldane system [1], [2], spin Peierls systems [3]–[5], and ladder spin systems [6], [7]. Nevertheless, the most studies have been performed on inorganic quantum spin systems [1]–[7]. However, the nonmagnetic impurity (NMI) effect on organic quantum spin system, exactly, on the organic ladder spin systems, was not evoked so much in the literature. Recently, S. Nishihara et al. [8] have reported the SQUID measurements of the magnetic susceptibility of $[Ph(NH_3)]([18]crown\text{-}6)[Ni(dmit)_2]$ showing that this later is a typical antiferromagnet S=1/2 two legs ladder spin system, where the magnetic moments are located on the $[Ni(dmit)_2]^-$ dimers (Fig.1). The NMI effect, corresponding to $[Au(dmit)_2]^-$ dimers, on this antiferromagnet has been studied showing that this compound remains S=1/2 two legs ladder spin system where the NMI affects the ladder system inducing some free spin moments which could correlate between them [8].

We have confirmed by CW-ESR spectrometer that the organic magnet, $[Ph(NH_3)](18\text{-crown-}6)[Ni(dmit)_2]$, is a good S = 1/2 two leg spin ladder antiferromagnetic system where the magnetic moments are located on $[Ni(dmit)_2]^-$ dimers. Therefore, we have investigated the nonmagnetic impurity effect, corresponding to $[Au(dmit)_2]^-$ dimers, concluding that these former could cut-off the spin ladder chain making some free induced spins of Ni (S=1/2). Depending on the distance between the induced Ni (S=1/2) spins, strong correlation between them could take place generating several systems with effective spin S=1 ferromagnetically coupled, while for infinite distance the induced spin Ni (S=1/2) becomes almost isolated on the quantum spin system.

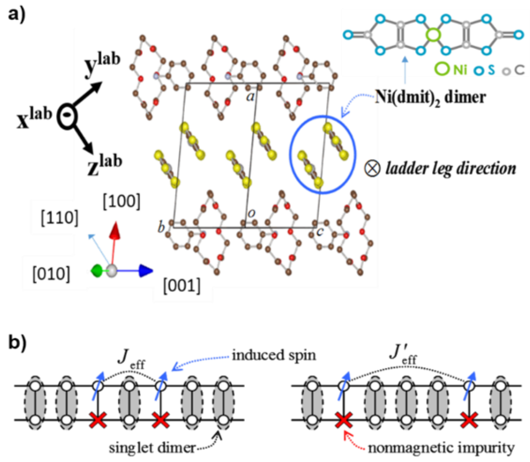

Figure 1 : **a)** Crystal structure of $[Ph(NH_3)]([18]crown\text{-}6)[Ni(dmit)_2]_{1-x}[Au(dmit)_2]_x$. The legs ladder direction is aligned along [011] crystal direction corresponding to X^{lab} axis. **b)** scheme of the spin ladder with defect induced by NMI.

References

[1] M. Yoshida *et al.*, *Phys. Rev. Lett.*, vol. 95, no. 11, Sep. 2005.
[2] Y. Uchiyama *et al.*, *Phys. Rev. Lett.*, vol. 83, no. 3, p. 632, 1999.
[3] M. Hase *et al.*, *Phys. Rev. Lett.*, vol. 71, no. 24, pp. 4059–4062, Dec. 1993.
[4] J.-P. Renard *et al.*, *Europhys. Lett. EPL*, vol. 30, no. 8, pp. 475–480, Jun. 1995.
[5] T. Masuda *et al.*, *Phys. Rev. Lett.*, vol. 80, no. 20, pp. 4566–4569, May 1998.
[6] M. Azuma *et al.*, *Phys. Rev. Lett.*, vol. 73, no. 25, p. 3463, 1994.
[7] M. Azuma *et al.*, *Phys. Rev. B*, vol. 55, no. 14, pp. R8658–R8661, Apr. 1997.
[8] S. Nishihara *et al.*, *Dalton Trans.*, vol. 42, no. 43, p. 15263, 2013.